https://doi.org/10.5194/egusphere-2024-4122
Preprint. Discussion started: 26 February 2025

Rockfall triggering and meteorological variables in the Dolomites (Italian Eastern Alps)

Francesca N. Bonometti [1], Giuseppe Dattola [1], Paolo Frattini [1], Giovanni B. Crosta [1]

[1]Department of Earth and Environmental Sciences - DISAT, Università degli Studi di Milano-Bicocca, Milano, 20126, Italy

Correspondence to: Francesca N. Bonometti (f.bonometti2@campus.unimib.it)

Abstract. Alpine areas are undergoing the highest change in temperature and rainfall intensity that represent main rockfall triggering factors. Since few approaches were proposed to analyse it, a new approach using meteorological variable frequencies was developed to comprehend climatic scenarios from 1970 to 2019 with implication on triggering historical rockfall events in the Dolomites.

The analysis considered key climate variables: mean air temperature, precipitation, thermal amplitude, freeze/thaw cycles and icing, under different aggregation scales. Results reveal that highest warming rates were observed during spring, while a notable reduction in icing and freeze-thaw cycles frequency was obtained during spring and autumn. An anticipation of both starting of summer and ending of winter was detected. Analyses with Rescaled Adjustment Partial Sums method provided valuable insights into precipitation long-term trends and fluctuations.

The analysis showed an increasing trend over last decade (2000-2019) suggesting variation in precipitation frequencies over years. The Bayesian method was employed to study conditional probability of meteorological variables on rockfall events. Rockfalls and high intensity rainfall are correlated in autumn, while with mean temperature at different altitudes in summer and autumn. Higher values probability of temperature amplitude characterises spring, while autumn seasons are interested to high temperature variation values. Finally, it was observed strong dependency of the freeze-thaw cycles and icing periods by regional timeseries.

1 Introduction

Rockfalls are a type of instantaneous collapse landslide, involving the detachment of a rock block (or several blocks) from a vertical or sub-vertical cliff, followed by rapid down-slope motion characterised by free-falling, bouncing, rolling, and local sliding phases (Varnes, 1978). These phenomena can involve a wide range of volumes and are extremely hazardous to human lives, structures, and infrastructures (Bunce et al., 1997; Crosta and Agliardi, 2004; Hilker et al., 2009; Volkwein et al., 2011; Zhao et al., 2017).

Various intrinsic and external parameters, highly variable over space and time, can trigger rockfalls (Volkwein et al., 2011), including earthquakes (Valagussa et al., 2014), intense rainfall (Palladino et al., 2018), snowmelt, permafrost degradation (Ravanel et al., 2017), freeze-thaw cycles (Matsuoka and Sakai, 1999), and ground temperature oscillations (Luethi et al., 2015; Palau et l., 2024; Stoffel et al., 2024), both in cold and warm conditions. Therefore, it is important to consider them when understanding the evolution of slopes in response to climate change and its impact on rock fall frequency and seasonality (Davies et al., 2001; Fisher et al., 2006; Stoffel and Huggel, 2012; Corò et al., 2015; Palau et al., 2024).

Climate change has caused a significant increase in temperature in mountain areas (Pepin et al., 2022) and the Alpine area over the last 150 years (Schär et al., 2004), with annual mean warming rates of about 0.5°C per decade since 1980 (Böhm et al., 2001; Allen and Huggel, 2013) beyond the average global changes. These changes are particularly impactful in the Alpine environment, leading to increase rockfalls. The effects of climate change in the Alpine area include: (i) potential temperature rise (Beniston, 2006; Brunetti et al., 2009; Gobiet et al., 2014), (ii) increased frequency and intensity of phenomena such as floods, droughts, rockfalls, and landslides (Gariano and Guzzetti, 2016; Palladino et al., 2017), and (iii) increased frequency

https://doi.org/10.5194/egusphere-2024-4122
Preprint. Discussion started: 26 February 2025

of medium and extreme precipitation events (Krautblatter and Moser, 2009), especially during autumn and winter (Schmidli and Frei, 2005).

A consequence of global warming is the increased degradation of permafrost (Noetzli et al., 2003; Gobiet et al., 2014; Draebing et al., 2019; Manent et al., 2024) in many steep rock slopes in high-mountain environments (Salzmann et al., 2007), which can affect slope stability at different scales. Gruber and Haeberli (2007) highlighted that warming air temperatures at high altitudes lead to permafrost degradation, affecting the stability of steep rock walls at different timings, magnitudes, and depths, as well as the thermal and hydraulic conditions of the rock mass. Davies et al. (2001) suggested that warming air temperatures alter the active layer thickness and fracture conditions, reducing rock mass shear strength (Krautblatter et al., 2013).

The effects of changing mean and extreme temperatures, and precipitation are likely to be widespread, influencing both the occurrence (in terms of temporal frequency) and the magnitude of future mass movements across the Alps. Therefore, it is necessary to analyse the relationship between meteorological variables and rockfall events. Many studies in the literature have demonstrated the relationship between rockfall occurrence and climate conditions in the Alpine environment. For instance, Frayssines and Hantz (2006) and D'Amato et al. (2016) found a correlation between rockfalls and freeze-thaw cycles, while Delonca et al. (2014) found a correlation with rainfall and minimum temperature. Seasonality also plays a role in rockfall occurrence, with Maciotta et al. (2015, 2017) noting the importance of freeze-thaw in early spring and Perret et al. (2006) observing a positive correlation between rockfall events and temperature in early summer. Studying a 100-year rockfall time-series, at a degrading slope in the Swiss Alps, Stoffel et al (2024) found that interannual and decadal trends indicate that rockfall activity correlates with summer air temperatures, and increases with warmer temperatures. This pattern, observed during the Early Twentieth Century Warming (ETCW) and since the mid-1980s, suggests that degrading permafrost contributes to slope instability and rockfalls, with interannual variations affected by other factors (e.g. snow cover, ground heat, and soil moisture).

To characterise the possible relationships between different climate variables and the triggering of slope failures, Paranunzio et al. (2015, 2016, 2019), Viani et al. (2020), and Paranunzio and Marra (2024) proposed a nonparametric method by analysing climate anomalies with different time aggregations associated with the events. Their method involves ranking all values of a climatic variable (V) recorded over the years in ascending order with a chosen scale aggregation. Each rockfall has n values of V_i, with i from 1 to n, associated with different years, where i is the i-th value of V in the ranked sample. The associated probability P(V) is calculated assuming variable V to be a significant triggering factor at an *alpha* level. This method links an extreme value of a climate variable with a rockfall event without considering their frequency.

The aim of this work is to calculate the frequency variation in time and space of different climate variables in the Italian Eastern Alps, to understand the climate evolution in the area and its influence on rockfall frequency distribution. To achieve this, a new method based on Paranunzio's methodology (2015) is proposed with improvements to address previous limitations regarding rockfall event frequencies, applying it to a large database of rockfall events in the study area.

This paper is organized as follows: Section 2 illustrates the study area and the collection of rockfall and climate data. Section 3 describes the method used for climate analysis and rockfall characterisation. Section 4 presents the results of the analyses. Section 5 discusses some issues with previous work. Finally, the conclusion reports on the correlation between climate change and rockfall events.

2 Case study

2.1 Study area

The study area, located in the eastern Italian Alps, spans 24.500km^2 and includes the Trentino-Alto Adige Region, and the provinces of Belluno (Veneto region), Pordenone and Udine (Friuli Venezia Giulia region). This area encompasses the Dolomites region, a group of carbonate platforms located in the eastern part of Southern European Alps, a south-vergent

https://doi.org/10.5194/egusphere-2024-4122
Preprint. Discussion started: 26 February 2025

Neogene thrust-and-fold belt, which constitutes a structural unit of the Alpine chain (Doglioni, 1987, Bosellini et al., 2003). The Dolomites are separated from the Austroalpine Unit by the Periadriatic Lineament, a major fault system of Oligocene-Neogene age. In the northernmost sector of the Bolzano Province (i.e., Aurina Valley), a little portion of the Tauern tectonic window is present, where the lower Penninic Unit crops out (Dal Piaz et al., 2003; Coro et al., 2015).

The bedrock consists of various lithologies, ranging from Permian terrigenous deposits including sandstone with conglomerates and dolostone with chalks (i.e., Val Gardena Sandstone, Bellerophon Fm.), to early Cretaceous carbonate rocks characterised by grey dolostone with oolites, breccias, limestone and claystone (i.e., Werfen Fm., Serla Dolostones, Contrin Fm., Marmolada Limestone, Sciliar Fm., Cassiano Dolostones, Raibl Fm., Dolomia Principale Fm.). These successions dominate in the province of Belluno, Trento, Pordenone and Udine. In the central part of the Trentino-Alto Adige region, the "Gruppo Vulcanico Atesino" consisting of volcanic rocks (pyroclastic flow, with subordinate domes and lavas), can reach a thickness of 2000m of. Additionally, in the province of Bolzano, micaschists, phyllites and gneisses are present, particularly to the north and northwest of the Periadriatic Lineament (Coro et al., 2015) (Figure 1).

The local morphology is primarily controlled by the geological and structural setting of the area, characterised by rock types with varying mechanical properties (Frattini et al., 2008). These rocks were initially severely folded or faulted and then uplifted during the various phases of the Alpine orogeny. Furthermore, the landscape was significantly reshaped during Pleistocene glaciations. Throughout the study area, the landscape is prominently marked by landforms (e.g., cirques and U-shape valleys) sculpted by the glacial tongues that occupied the region during the Last Glacial Maximum (LGM) and retreated to the highest valleys during the Late glacial period (Bassetti and Borsato, 2015).

2.2 Data collection

To analyse the climate variation and its relation with rockfall events, as reported in Sect. 3, a complete record of meteorological variables and rockfall data is required. The descriptions and methods used to obtain these data are detailed below.

2.2.1 Meteo-climatic time-series

Time-series of meteorological data from weather stations were collected from the SCIA website (https://scia.isprambiente.it/). Some weather stations were excluded to ensure a homogeneous dataset; only weather stations containing complete daily time-series of climatic variables were considered. Consequently, 277 out of 1244 weather stations were selected (Fig. 1). The chosen climatic variables included total daily rainfall, daily minimum temperatures, and daily maximum temperatures. The daily time-series spanned from January 1, 1970, to December 31, 2019.

A dataset for each climatic variable was generated, containing: (i) an identification code for the stations, (ii) their coordinates, and (iii) their daily values of climatic variables.

2.2.2. Rockfall catalogue

A new rockfall dataset was created from 5503 events extracted from various sources: (i) 5317 from the Italian Landslide Inventory project (IFFI https://idrogeo.isprambiente.it/), (ii) 102 rockfalls from the Geomorphological impacts of Climate change in the Alps (GeoClimAlp https://geoclimalp.irpi.cnr.it/) database, (iii) 18 from the Rete Ferroviaria Italiana (RFI) dataset, and (iv) 66 from online news sources. To establish a correlation between climatic variables and rockfall events, it is essential to have information on the day, month, and year of occurrence. Therefore, out of 5503 events, 2971 with complete date information were considered (Fig. 1). A comprehensive dataset was generated, including: identification code (ID), coordinates (x, y, z), date of event (dd/mm/yyyy), and the associated three closer weather station.

https://doi.org/10.5194/egusphere-2024-4122
Preprint. Discussion started: 26 February 2025

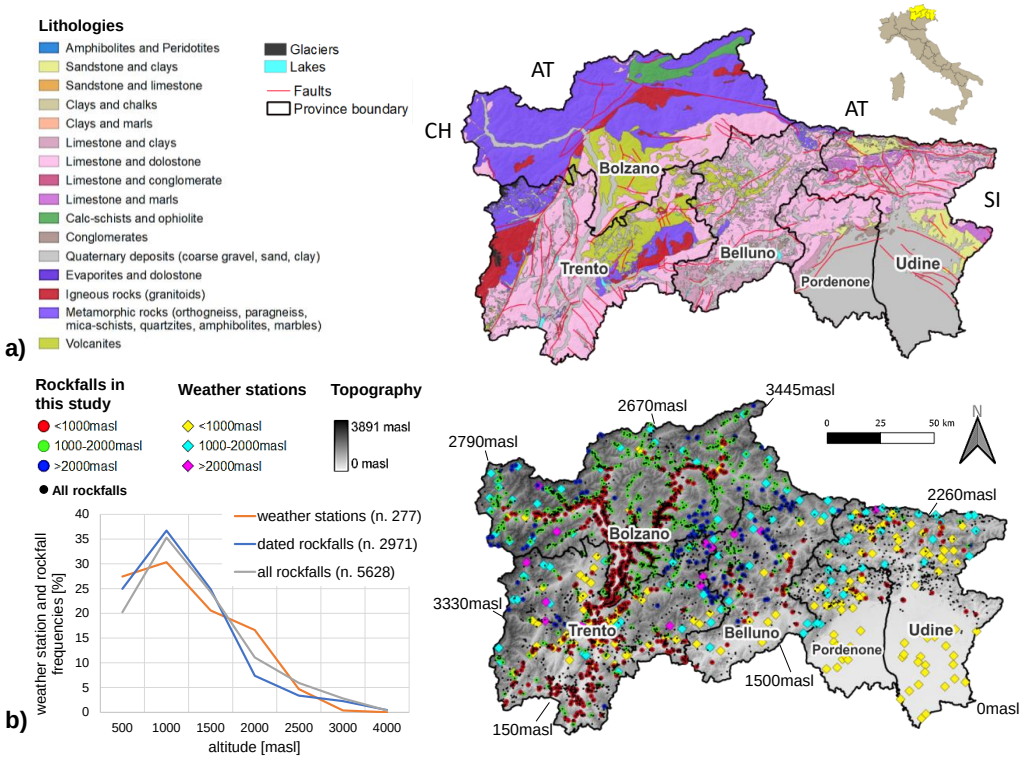

Figure 1: (a) Geological setting of the study area (lithology modified from regional open source data). (b) Location and distribution according to altitude of 277 weather station (diamonds), 5628 rockfall data (black dots) and 2971 dated rockfall events (dots) used in the analyses. Meteorological stations: 87 in Trento Province, 46 in Bolzano Province, 30 in Belluno Province, 37 in Pordenone Province and finally 77 in Udine Province. The monitoring network considerated from SCIA are: Idrografica, Regionale and Sinottica. Rockfall events are located: 403 in Trento Province, 2391 in Bolzano Province, 130 in Belluno Province, 9 in Pordenone Province and 29 in Udine Provinces.

3 Methods

The proposed method involves assessing both the variation of climatic conditions in an area and the effects of this variation on rockfall occurrence. In this analysis, the frequency of meteorological data is computed by extrapolating from the meteo-stations' time-series to create a sampled time-series, using a procedure discussed in the following sub-sections. Differently from Paranunzio et al. (2015, 2016), which identified anomalies in the analysed meteorological variables, this method focuses on the frequency of meteorological variables within their characteristic values ranges.

The *measured meteorological variables* from the weather station employed in this study were the same as in Paranunzio et al. (2015, 2016), namely daily minimum air temperature T_0, daily maximum air temperature T_1, and daily precipitation R.

The *derived meteorological variables* included daily mean air temperature, T_m, and daily air temperature amplitude, $T_a = (T_1 - T_0)$. To analyse the effects induced by both freeze/thaw cycles and icing, two Boolean variables were introduced: freeze/thaw cycle, C_{FT}, which is 1 if the cycle occurs ($T_0 \leq 0$°C and $T_1 > 0°C$), and icing, I, which is true if both T_0 and T_1 are negative. These derived climatic variables were chosen based on previous studies indicating their potential to trigger rockwall instabilities in alpine environment (Douglas, 1980; Sandersen et al., 1996; Matsuoka and Sakai, 1999; Frayssines and Hantz, 2006; Letortu 2013; d'Amato et al., 2015; Maciotta et al., 2017).

https://doi.org/10.5194/egusphere-2024-4122
Preprint. Discussion started: 26 February 2025

3.1 Computed time-series of meteorological variables

Since the time-series of aforementioned variables refer to daily measurements, the effects of multi-day quantities cannot be directly obtained from them. To overcome this limitation, *computed time-series* (obtained from the original data through various computational methods) were derived using the following procedure, which considers multi-day effects (aggregation scale, S_a). Let us consider a time series of one of the above-mentioned meteorological variables:

$$(D_i, V_i) \quad i = 1, \cdots, n_t \tag{1}$$

where V_i is the meteorological variable value, D_i is the date, and n_t is length of the time-series (i.e., the number of values of reported in the time-series). It is possible to derive the computed time-series using three basic procedures: mean, addition and subtraction.

In case of the mean procedure, the new time-series can be obtained by computing the average following Eq.(2):

$$\bar{V}_i = avg\left(\left[V_{i-S_a}; V_i\right]\right) \quad i = \mathrm{S_a}, \cdots, n_t \tag{2}$$

where avg is the average operator, $\bar{V}_i$ is mean of the values within the closed interval $\left[V_{i-S_a}; V_i\right]$. Consequently, the mean time-series has the following form:

$$(D_i, \bar{V}_i) \quad i = \mathrm{S_a}, \cdots, n_t \tag{3}$$

In case of addition the new values are computed as indicated in Eq. (4):

$$V_i^a = \sum_{j=1}^{S_a-1} V_{i+1-S_a+j} \quad i = \mathrm{S_a}, \cdots, n_t \tag{4}$$

and the new time-series has the form expresses in Eq. (5):

$$(D_i, V_i^a) \quad i = \mathrm{S_a}, \cdots, n_t \tag{5}$$

Finally, in the subtraction procedure, the new values are computed using the following formula:

$$\Delta V_i = V_i - V_{i-S_a} \quad i = \mathrm{S_a} + 1, \cdots, n_t \tag{6}$$

and the new time-series has the form:

$$(D_i, \Delta V_i) \quad i = \mathrm{S_a} + 1, \cdots, n_t \tag{7}$$

For the C_{FT} and I time-series, the computed time-series coincides with the original ones since no aggregation scale is considered for these variables.

3.2 Sampled time-series

Once the computed time-series were obtained, the sampled time-series were derived from them using the reference date set D_r and the temporal scale S_t. Denoting D_e a chosen date the set of reference dates $\boldsymbol{D}_r$ set is defined with Eq. (8):

$$\boldsymbol{D}_r = \{D_i \mid D_i = D_e + k365days\} \tag{8}$$

This set contains the chosen date and the corresponding dates with same day and month but different years of the chosen date. The number of years used for the analysis depends on the computed time-series dates. The sample time-series is obtained from the computed time-series using the following condition:

$$(D_i, V_i^s) = (D_i, V_i^c) \quad D_i \in [D_r - S_t; D_r + S_t] \tag{9}$$

in which $D_r \in \boldsymbol{D}_r$ are the reference dates and V_i^c is the value of the computed time-series according to the procedures proposed in the previous sub-section and V_i^s is the value of sample time-series.

https://doi.org/10.5194/egusphere-2024-4122
Preprint. Discussion started: 26 February 2025

3.4 Bayesian method

The influence of a weather variable on rockfall events can be analysed using the Bayesian method (Bayes. 1763), to obtain the conditional probability of a meteorological variable to act as a trigger for a rockfall (Berti et al., 2012). Consider a time series of a meteorological variable, with its range divided into intervals. Let R represents the set of rockfall events under analysis, and M_i the set of recorded data within a specific $i-th$ interval. The probability can be obtained as follows:

$$P(R|M_i) = P(M_i|R)\frac{P(R)}{P(M_i)} \quad (10)$$

where $P(R|M_i)$ is the probability that rockfall events are conditioned by the meteorological variable within the range $i-th$, $P(R)$ is the rockfall probability, $P(M_i)$ is the probability of the meteorological variable falling within the $i-th$ range, and finally, $P(M_i|R)$ is the probability of the meteorological variable being in the $i-th$ interval when a rockfall event occurs.
To apply this method to the aforementioned variables, a time series of the selected meteorological variable for the area under consideration must be used. This involves averaging the time-series from all considered stations. For each day of the measurement interval, the value of the meteorological variable is the mean of the values from all stations included in the analysis. After processing this new time-series with the proposed approach, a sample time-series is obtained, which is then used in the Bayesian method. For the case of icing and freeze/thaw time-series, the maximum and minimum temperatures were considered, taking into account both spatial mean, maximum and minimum values.

3.5 Climate analysis

Considering all the meteo-stations in the area those with time-series covering a range of five decades were selected. To perform a climate analysis, the World Meteorological Organization (WMO) establishes the *climatological standards*, (WMO, 1989) namely averages of climatological data computed for consecutive periods of 30 years. They also introduce *provisional normals* (WMO, 1989), which are short period means based on observations extending over at least ten years at continental or global scales. Based on this consideration, a ten-year interval was deemed sufficient for the restricted area considered in this study. Therefore, meteo-stations with complete time-series from 1970 to 2019 were chosen for the following analyses.
The above procedure was employed to obtain both the calculated and sampled time-series using an aggregation scale $S_a = \{0,7,30,90\}$ and a temporal scale $S_t = 45$ days. For the C_{FT} and I variables, the time scale $S_t = \{15,45\}$ was used. The results were grouped into five decades, and for each decade, the values for each variable were divided into ten bins, and the corresponding frequencies were computed. For the C_{FT} and I variables, the frequency of persistence was computed, where the persistence of C_{FT} and I were defined as the number of continuous days in which C_{FT} and I are respectively true. The aim of this computation was to check the variations in the frequency of each variable over time.

3.6 Rockfall and climate indices

The aforementioned method requires the time-series of the meteorological variables as input. However, the location of the rockfall event differs from that of the meteo-stations, and consequently, the meteorological time-series for that precise point is not known. Therefore, this time-series was derived from the time-series recorded at the meteo-stations using two methods.
The first methods involve assessing the distance between the meteo-stations and the rockfall event source, selecting the time-series associated with the closest meteo-station, as follows:

$$V_{rf}(t) = V_n(t) \quad (11)$$

where $V_{rf}(t)$ is the rockfall source time-series and the $V_n(t)$ is the time series for the closest time-series weather station. This method is the same as that employed by Paranunzio et al. (2015). This approach does not account for the fact that meteorological variables change according to (i) elevation and (ii) spatial location. These variations are significant because

https://doi.org/10.5194/egusphere-2024-4122
Preprint. Discussion started: 26 February 2025

weather stations and rockfall sources have different elevations and spatial locations. Therefore, the time series from weather stations may not be representative of the rockfall source site. To address this issue, the following procedure was used in this study. First, the weather station points were connected by a Delaunay triangulation that considers only horizontal coordinates. Consequently, the rockfall source point belongs to one of the triangles of the Delaunay triangulation. The vertices of the triangle are three weather stations, referred to as nodal weather stations, associated with that rockfall event source. The time series from these nodal weather stations were used to calculate the time series at the rockfall event source.

To obtain the rockfall site weather time-series, two corrections were employed. The first correction, the altitude correction, involved adjusting the temperature time-series values using the following mathematical expressions Eq. (12):

$$V_i^*(t) = V_i(t) - c\left(z_{rf} - z_i\right) \tag{12}$$

where $V_i(t)$ is the variable value recorded by the nodal weather stations, z_i is the nodal weather elevation, z_{rf} is the rockfall elevation, c is the vertical gradient correction, and $V_i^*(t)$ are the corrected weather variable values. According to (Stull, 2000) $c = 0.0065°\text{C/m}$.

The spatial correction involves computing the site weather time-series according to the following relationship:

$$V_{rf}(t) = N_1(x,y)V_1^*(t) + N_2(x,y)V_2^*(t) + N_3(x,y)V_3^*(t) \tag{13}$$

where $N_i(x,y)\ i = 1,2,3$ are the weight functions depending on the weather stations's positions, and (x,y) the coordinates of the rockfall event source. The weight functions, ranging between 0 and 1, were computed by imposing a linear interpolation between the weather stations' values according to their spatial positions. This correction was applied to temperature and rainfall variables. Figure 2 provides a schematic representation of the rockfall source, P, and the surrounding weather stations.

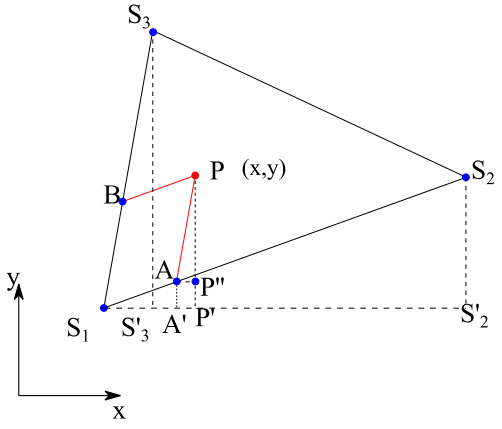

Figure 2: Schematic representation of the rockfall source point P and the weather stations (S_1, S_2 and S_3) positions forming a triangle used int time-series computations.

Once $V_{rf}(t)$ was computed for all meteorological variables, computed time-series and sampled time-series were attained.

4 Results

Rockfall events are initiated by various mechanisms that generate rock mass degradation, which in turn leads to a progressive reduction in rock mass strength, particularly in areas with steep slopes and sparse vegetation, or with permafrost. This study focuses on the effects of meteorological variables in triggering rockfall events. Over the decades, observed changes in climate conditions have led to variations in meteorological variables, thereby altering degradation rates and the probability of triggering rockfalls. Consequently, this affects the temporal and spatial distribution of rockfall events. Using the method proposed in the Sect. 3, the following analysis demonstrates the impact of climate change on rockfall events.

https://doi.org/10.5194/egusphere-2024-4122
Preprint. Discussion started: 26 February 2025

Eighteen stations out of the total 277 were selected for the climate analysis, based on those with the longest records covering the period from 1970 to 2019. The results are presented for mean air temperature and precipitation at a 90-day aggregation scale, while a 7-day aggregation scale was used to assess the frequency of freeze-thaw cycles. This choice was made to observe detailed short-term changes and avoid overlap with other months. Additional results are provided in the supplementary materials for completeness (S1). The analysis of rockfall events was performed using data from all 277 stations. The frequency of climate variables associated with rockfall events is shown for an aggregation scale of 0 days, while results for other aggregation scales are reported in the supplementary materials (S2).

4.1 Climate analysis

4.1.1 Rainfall

Rainfall is a significant triggering factor for rockfalls, especially when its intensity is very high, as water infiltrates into rock mass discontinuities, affecting both the onset of rockfalls (Delonca et al., 2014; Palladino et al., 2018) by increasing water pressure, the melting of ice in fractures, the erosion of discontinuity fillings, and the dissolution of cementing materials (Nissen et al., 2022).

The evolution of rainfall over different decades, seasons, and at a 90-day aggregation scale was analysed, and the results in terms of frequency are reported in Fig. 3. Apart from fluctuations between different decades, particularly above 2000 meters of elevation during spring (shown in supplementary materials, Fig.S2), the frequency of low and high rainfall intensity events decreases and increases, respectively. The largest increase in high-intensity frequencies occurs during winter and autumn seasons. This behaviour becomes more evident with increasing aggregation scale, as three months of accumulated rainfall are added up (see the results of other aggregation scales in the supplementary materials, S1.1).

https://doi.org/10.5194/egusphere-2024-4122
Preprint. Discussion started: 26 February 2025

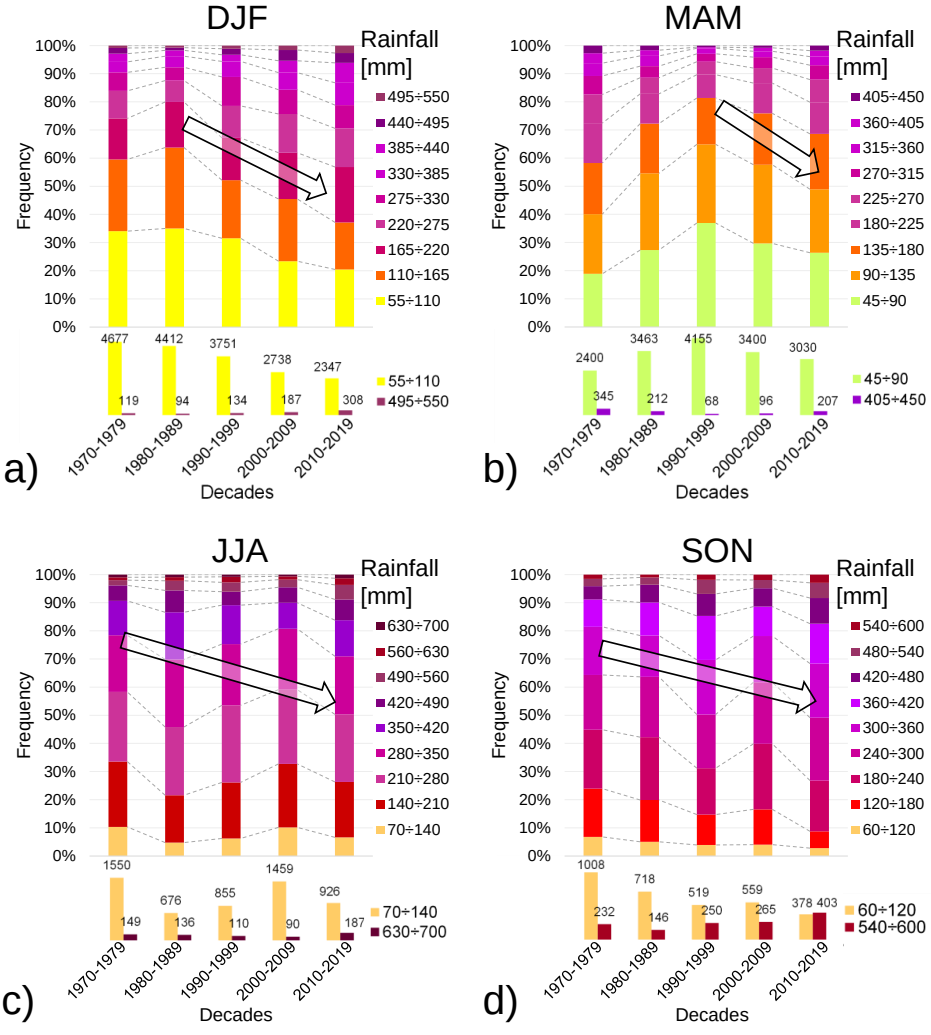

Figure 3: Frequency distribution of accumulated rainfall with an aggregation scale of 90 days considering all altitudes during (a) winter (DJF), (b) spring (MAM), (c) summer (JJA) and (d) autumn (SON). The arrow illustrated a possible trend. For each graph, frequencies of maximum and minimum ranges are zoomed in in the bottom.

4.1.2 Air mean temperature

Air temperature varies yearly, seasonally, monthly, and daily, with weather stations recording the maximum and minimum daily temperatures. The onset of a rockfall can be associated with temperature variations during the day and over time. For the purpose of this analysis, the variation of temperature over time (longer than one day) is represented by mean air temperature, while within a day, air temperature amplitude is used.

In Figure 4, the frequencies of the mean temperature at a 90-day aggregation scale are reported for the four seasons, five decades, and all altitudes. A reduction in the frequency associated with low temperatures and an increase in the frequency of high temperatures is observed over the decades. For all seasons and at all altitudes (see supplementary materials, S1.2), the results indicate a slight warming trend in the study area, with a significant frequency increase during the autumn season.

https://doi.org/10.5194/egusphere-2024-4122
Preprint. Discussion started: 26 February 2025

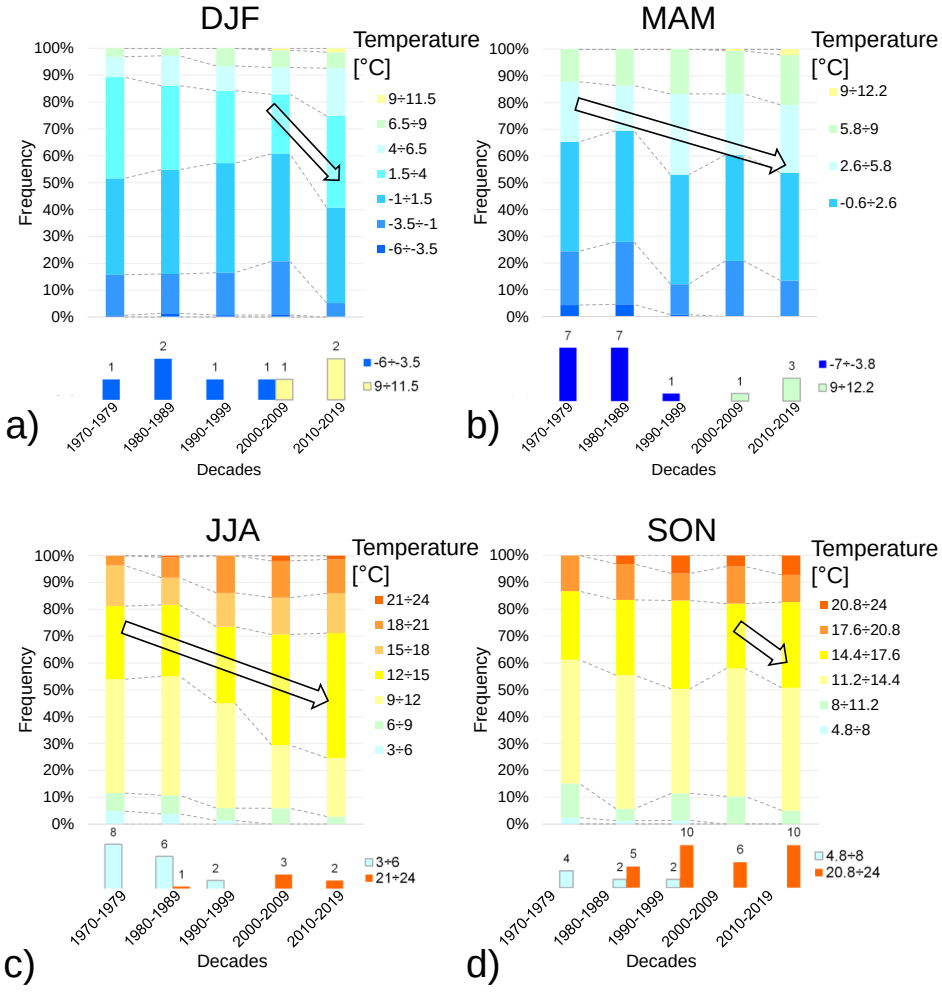

Figure 4: Frequency distribution of mean temperature with an aggregation scale of 90 days considering all altitudes during in the following seasons: (a) winter (DJF), (b) spring (MAM), (c) summer (JJA) and (d) autumn (SON). The arrow illustrated a possible trend. For each graph, frequencies of maximum and minimum ranges are zoomed in in the bottom.

4.1.3 Temperature variation

Air mean temperature variation, defined as the difference between the air mean temperature on a given day and the corresponding air mean temperature assessed on a preceding day chosen according to the aggregation scale. In Figure 5 frequencies of temperature variation with an aggregation scale of 6 days for the four seasons are shown. No significant changes in temperature variation over the decades are evident, except for some slight fluctuations. Therefore, temperatures over the years change gradually from on season with the subsequent one keeping the same evolution across all decades. This conclusion is consistent when considering other aggregation scales, as shown in the supplementary materials (S1.3). Comparing the highest and lowest values of ΔT, an increase in the range between 8÷10°C during winter in the last decade was observed (Figure 5a). In summer, a reduction of frequencies of extremes values was observed (Figure 5c).

https://doi.org/10.5194/egusphere-2024-4122
Preprint. Discussion started: 26 February 2025

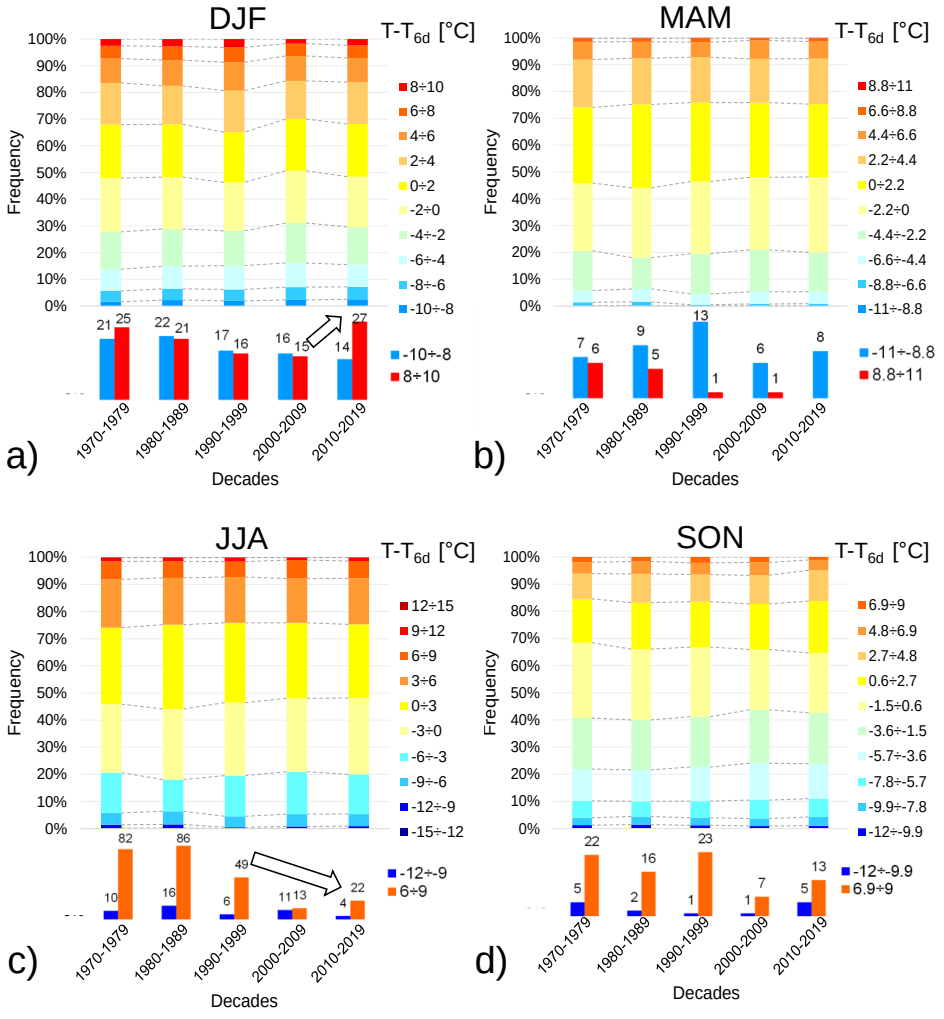

285 **Figure 5: Frequency distribution of mean temperature difference with an aggregation scale of 6 days at all elevations during in the following seasons: (a) winter (DJF), (b) spring (MAM), (c) summer (JJA) and (d) autumn (SON). The arrow illustrated a possible trend. For each graph, frequencies of maximum and minimum ranges are zoomed in the bottom.**

4.1.4 Temperature amplitude

The results concerning temperature amplitude frequencies, considering different decades and seasons, are shown in Figure 6.
290 In all seasons, except winter, an increase in the frequencies of maximum temperature amplitude and a reduction in the lowest range frequencies were observed. This indicates that on many days, there can be a significant difference between the minimum and maximum temperatures, averaging 11°C. Conversely, during the winter season, the opposite trend was observed: low temperature amplitude ranges increased, while high ones decreased over the last decade. This suggests that there is not much difference between minimum and maximum temperatures in winter.

https://doi.org/10.5194/egusphere-2024-4122
Preprint. Discussion started: 26 February 2025

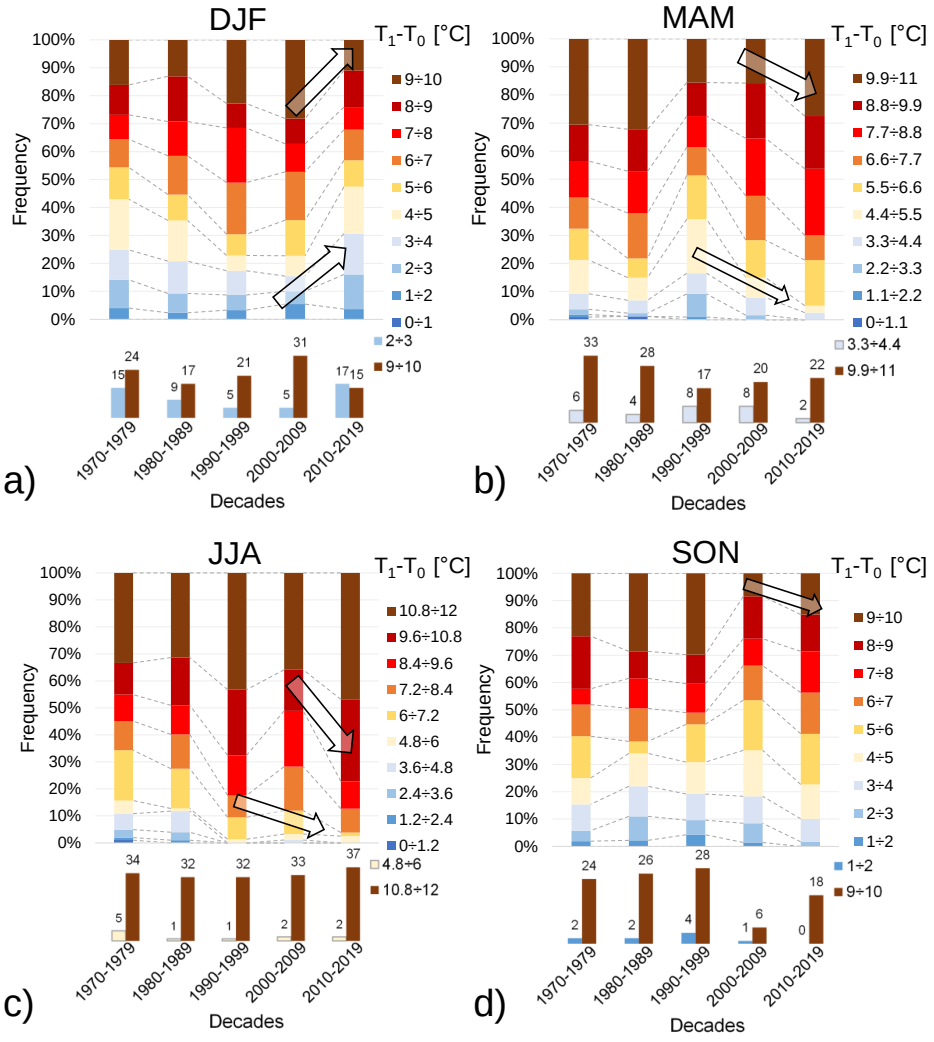

Figure 6: Frequency distribution of daily air temperature amplitude at all elevations during in the following seasons: (a) winter (DJF), (b) spring (MAM), (c) summer (JJA) and (d) autumn (SON). The arrow illustrated a possible trend. For each graph, frequencies of maximum and minimum ranges are zoomed in the bottom.

4.1.5. Freeze-Thaw cycle

As the frequencies of high temperatures increase, the number of days with maximum and/or minimum daily temperatures above zero also rises. This alters the persistence of icing in the area, affecting the onset of the freeze/thaw cycles, and increasing the number of days with no ice. Specifically, freeze/thaw cycles accelerate the rock mass degradation processes by reducing cohesion at the ice-rock interface. To study these effects, the persistence of the icing and freeze/thaw cycles were analysed, with results for freeze/thaw cycles shown in Figure 7, considering different elevations at a 7-day aggregation scale. For each elevation, two months were considered, as these are when freeze/thaw cycles either stop or begin.

The results indicate that, in general, the persistence and frequency of freeze-thaw cycles have decreased over the years. This means the number of consecutive days with freeze/thaw cycles has reduced. Analysing different altitude ranges, for elevations below 2000m (Figure 7a, b, c and d), this reduction in persistence is observed in March/April and October. Due to warming, high frequencies with low persistence are observed in March/April in the last decade, as freeze/thaw cycle days are not

https://doi.org/10.5194/egusphere-2024-4122
Preprint. Discussion started: 26 February 2025

consecutive. Similarly, in October at low altitudes (Figure 7b), freeze/thaw cycles occur less frequently and tend to disappear. At medium altitudes between 1000m and 2000m (Figure 7c and d), an increase in frequencies with one day persistence is recorded, indicating that freeze/thaw cycles are becoming more discontinuous, separated by days with minimum temperature above zero. Above 2000m (Figure 7e and f), a significant decrease in cycle frequency is observed in June and September. In September, many frequencies of consecutive days of freeze/thaw cycles with low persistence (2 days) are noted. In past decades, freeze/thaw cycles were less frequent but more continuous. These variations across different elevations are due to the linear decrease in temperature with increasing altitude, which delays summer and advances winter at higher elevations. Similar patterns can be observed at other aggregation scales, as shown in the supplementary materials (S1.5).

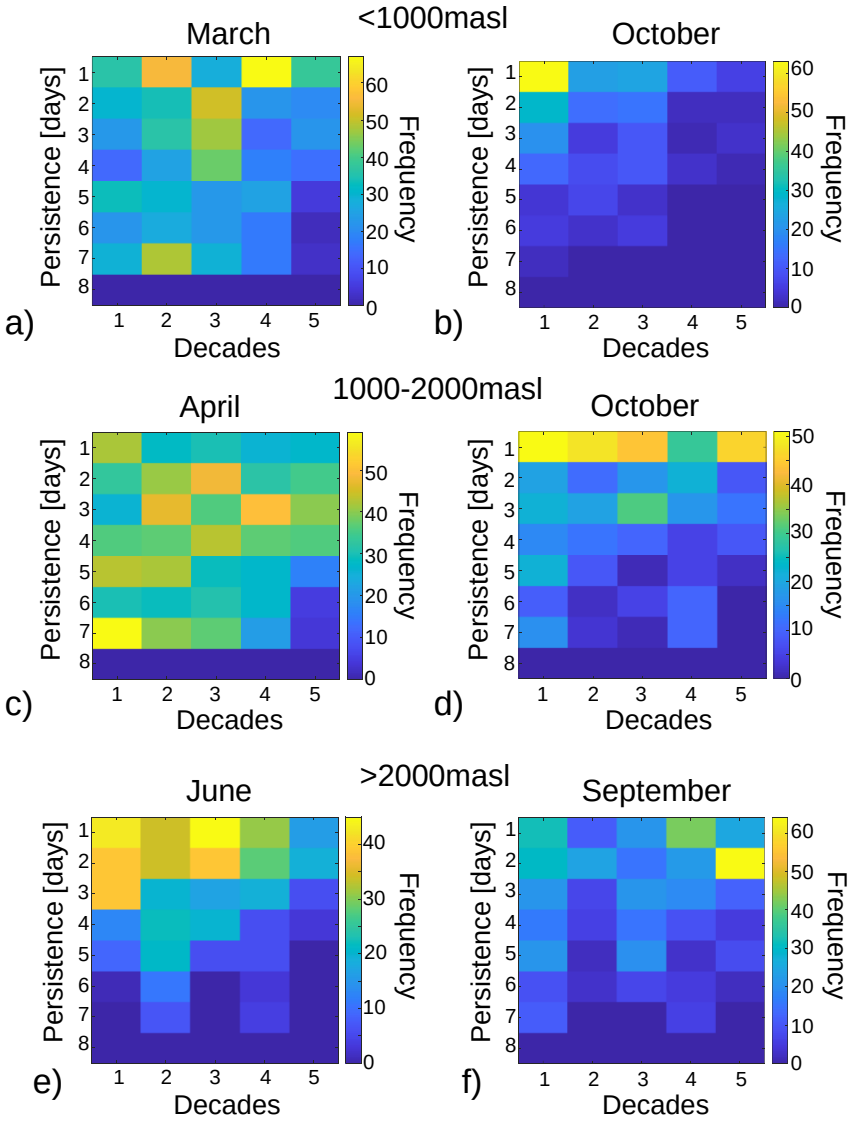

Figure 7: Heatmaps of freeze-thaw cycle frequency during thawing and freezing period: (a-b) below 1000m asl, (c-d) between 1000m-2000m asl and (e-f) above 2000m asl.

https://doi.org/10.5194/egusphere-2024-4122
Preprint. Discussion started: 26 February 2025

4.1.6 Icing

Figure 8 shows the persistence of icing for the spring and autumn seasons at elevations above 2000m, using a 7-day aggregation scale. Lower elevations are not considered, as no relevant icing phenomena are present at these altitudes in the studied decades. The results indicate that in April and November, there is only a reduced frequency of 7-day persistence. In April and October, there is an increase in 1-day persistence, while in May, a reduction in persistence is noted. Consequently, the variation in frequencies implies that the total number of icing days changes slightly, but they are interspersed with days without ice. This phenomenon is primarily due to an increase in maximum daily temperatures which causes a transition from icing to freeze/thaw cycles. To verify this transition, Figure 9 plots the persistence of freeze/thaw cycles for the same months and aggregation scale. A global increase in the frequency and persistence of freeze/thaw cycles is observed, indicating that some icing days are converted into freeze/thaw cycles days.

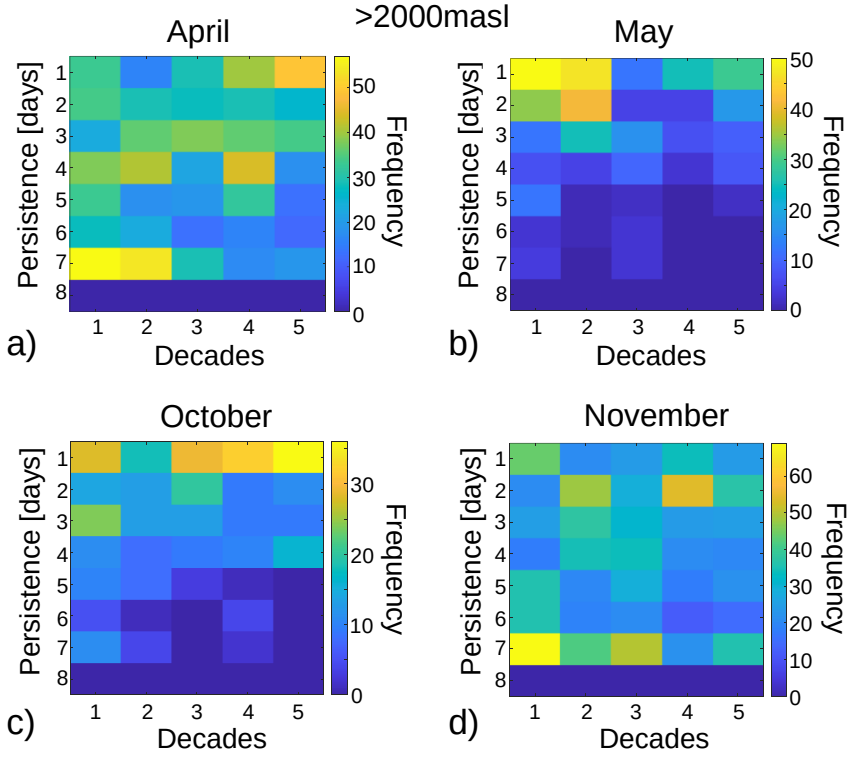

Figure 8: Heatmaps of icing frequency above 2000m asl: during (a-b) spring season and (c-d) autumn season.

https://doi.org/10.5194/egusphere-2024-4122
Preprint. Discussion started: 26 February 2025

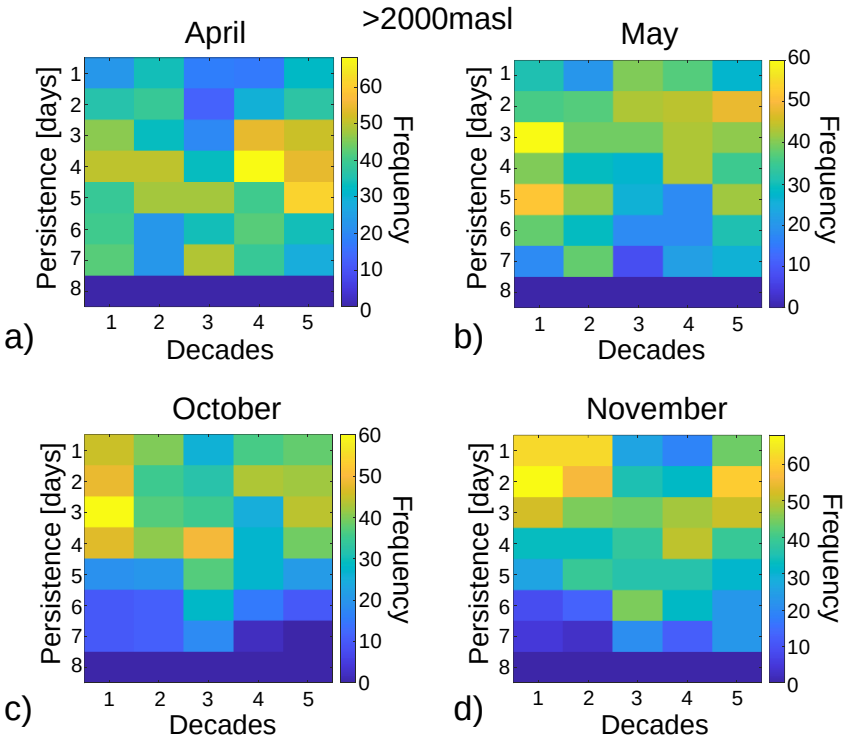

Figure 9: Heatmaps of freeze-thaw cycle frequency above 2000m during (a-b) spring season and (c-d) autumn season.

4.2 Rockfall events distribution

From the dataset of 5480 rockfalls occurred between 1970 and 2019, 2971 rockfalls were extracted for analysis. The results obtained by the proposed approach are discussed below.

In Figure 10a, the number of recorded rockfall events is shown alongside the number of active weather stations. The graph suggests an increase in rockfall frequency over the past two decades. However, as highlighted by Huggel et al., (2012), Sass and Oberlechner (2012), Rupp and Damm (2020) and Bajni et al. (2021), this increase could be attributed to improvements in the accuracy, completeness and the level of documentation at all elevations and for all rockfall events in recent years.

Figure 10b shows the monthly frequency revealing three main peaks in November, February-March-April and August. The altitudinal distribution of rockfalls events (Figure 10c) shows a concentration below 1500m each year. For elevations above 1500m, an increase in frequency is observed over the decades. However, in recent decades, a relative decrease is noted below 1000m, while a relative increase is observed above 1500m. Regarding the aspect of the rockfall source (Figure 10d), 70% of events below 1000m occur on broadly south-facing slopes. In contrast, 50% of rockfalls above 2000 meters occur on north-northwest facing slopes, and 35% of events between 1000 and 2000 meters occur on south-southeast facing slopes. Above 2000m, this pattern can be attributed to permafrost thawing, which predominantly affects higher elevations on north-facing cliffs (Noetzli et al 2003, Noetzli and Gruber 2009).

https://doi.org/10.5194/egusphere-2024-4122
Preprint. Discussion started: 26 February 2025

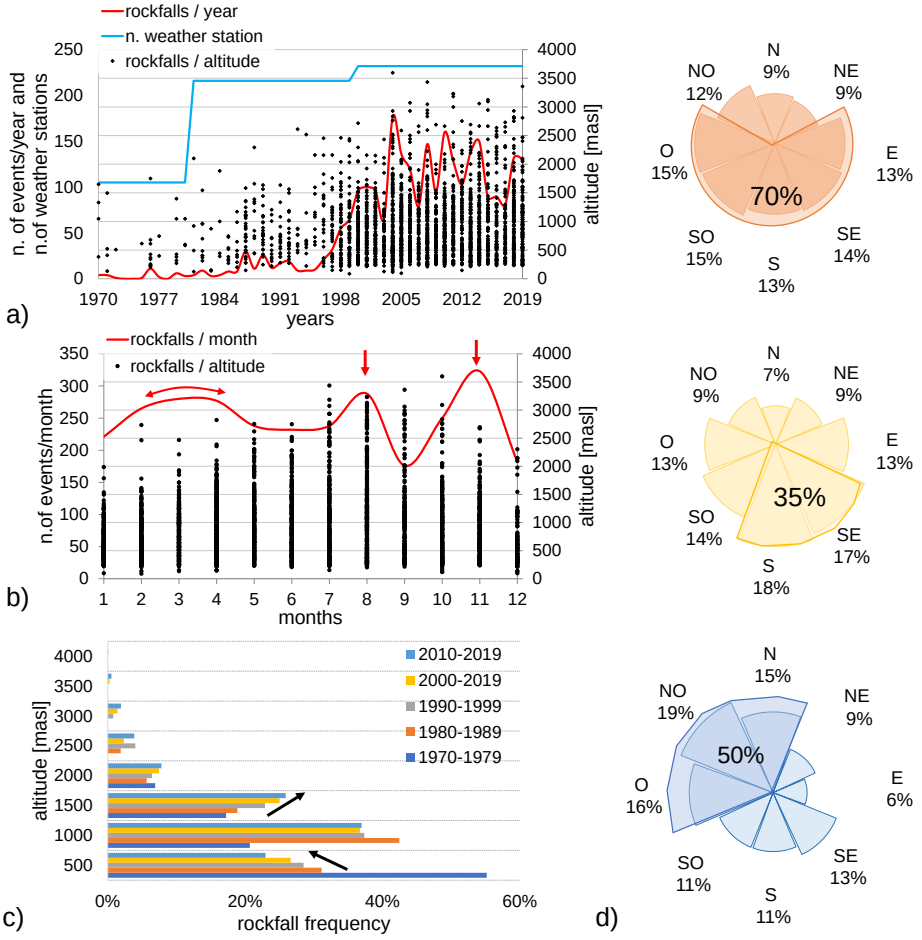

Figure 10: Analysis of 2971 rockfall events from 1970 to 2019: (a) distribution of annual frequency of rockfalls regarding to altitude, the red line is the number of rockfalls/year and blue line the number of active weather stations; (b) monthly frequency of rockfall events regarding to altitude for all years, the red line is the number of rockfalls/month; (c) rockfall events distribution in terms of altitude and decades; (d) frequency of rockfall occurrence in terms of aspect classes and for different altitudes.

4.3. Rockfalls and climate variables

The aim of this sub-section is to assess the correlation between rockfall events and weather variables. Since weather variables vary over time and space, the analysis was presented in terms of elevation range, season, and aggregation scale. The same climate variables used in the climate analysis were considered, using the same ranges. For simplicity, only the more important results were illustrated here, while tables containing all conditional probability analysed are shown in supplementary materials (S2).

4.3.1 Rainfall

Figure 11 shows the conditional probabilities of cumulative rainfall obtained from weather stations below 1000masl for the autumn season with $S_a = 90$, while Figure 11a and Figure 11b for autumn season between 1000-2000masl with $S_a = 30$. In these two cases an increment of conditional probability for the values with highest intensity of rainfall, are shown in the last decade; with 12.4% below 1000m and 22.2% between 1000-2000m of probability. Observing results with other aggregation scale and altitudes, highest probabilities with rainfall are present again during autumn season with an aggregation scale of 7

https://doi.org/10.5194/egusphere-2024-4122
Preprint. Discussion started: 26 February 2025

days below 2000m and with daily aggregation scale below 1000m. Therefore, for high rainfall values in the autumn season there could be a correlation between rockfall events and high intensity rainfall. Furthermore, it is noted that in the past rockfalls had a probability of occurrence with a daily and weekly aggregation scale, whereas in the last decade the probabilities are higher with a monthly and quarterly aggregation scale.

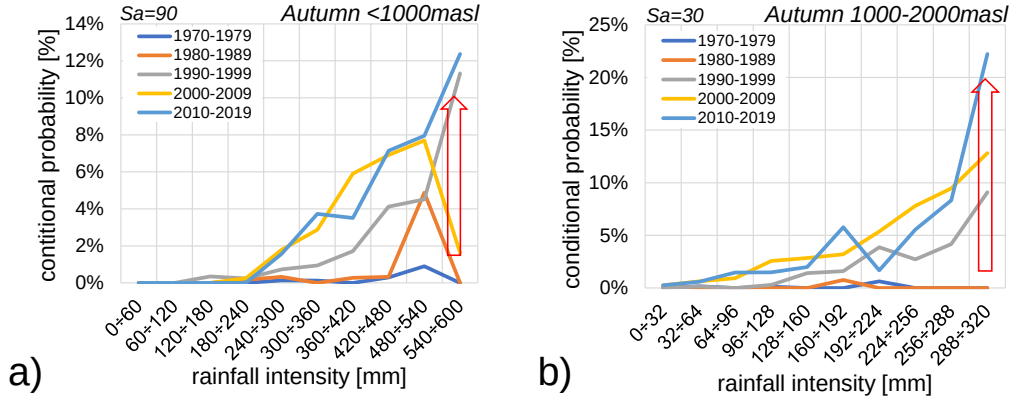

Figure 11: (a) Conditional probabilities of rockfalls triggers by rainfalls from 1970 to 2019 during autumn season. (a) below 1000m considering an aggregation scale $S_a = 90$. (b) between 1000-2000m considering $S_a = 30$.

4.3.2 Mean air temperature

Figure 12a show a conditional probability of 12.7% of mean weekly air temperatures at elevations between 1000-2000m for the summer season. Figure 12b illustrates probability of 2.2% of rockfall event by monthly temperature above 2000m during autumn season. Analysing all results in the supplementary materials (S2.2), rockfall probability increased during decades particularly in the last two decades with higher probabilities in winter and spring below 1000m, in summer between 1000m and 2000m and in autumn above 2000m. These results imply a possible correlation between rockfall events and increasing temperatures in accordance to climate analysis.

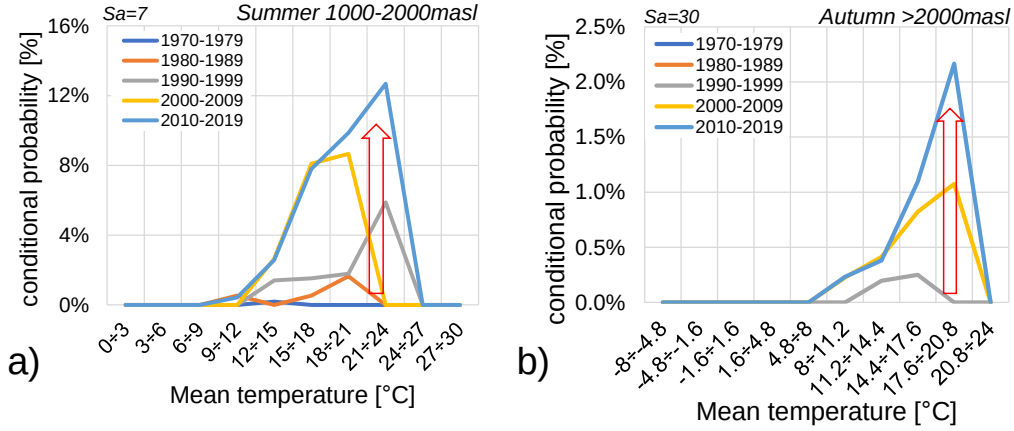

Figure 12: (a) Conditional probabilities of rockfalls triggers by mean temperature values from 1970 to 2019 during summer season between 1000-2000m considering an aggregation scale $S_a = 7$. (b) Conditional probabilities of rockfall from 1970 to 2019 during autumn season above 2000m.

4.3.3 Temperature amplitude

In Figure 13 the conditional probabilities of monthly air temperature amplitude ($Tmax - Tmin$) during (a) spring season below 1000masl and (b) winter season between 1000masl and 2000masl are presented. Observing Figure 13a, 28.6% of

https://doi.org/10.5194/egusphere-2024-4122
Preprint. Discussion started: 26 February 2025

probability correspond to range of temperature amplitude 8.8°C to 9.9°C. Figure 13b shows a 5.8% of probability that rockfall are conditioned by temperature amplitude with a range of 9°C to 10°C. All results present higher values of probability in the last two decades with temperature amplitude ranges greater than 6.6°C during spring and range from 9°C to 10°C in winter, except with $Sa = 0$. So higher probabilities are found with highest ranges of temperature amplitude.

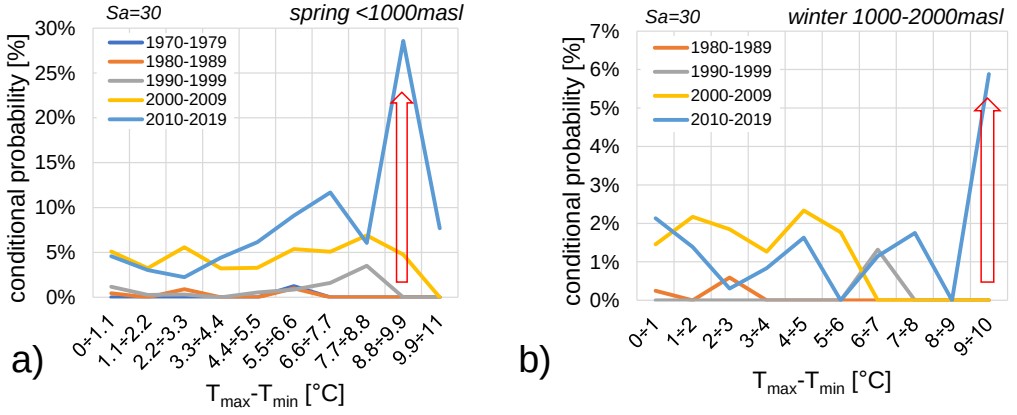

Figure 13: Conditional probabilities of rockfalls conditioned by ranges of temperature amplitude from 1970 to 2019. (a) during spring season below 1000m and (b) during winter season between 1000m-2000m.

4.3.4 Air mean Temperature variation

In Figure 14 the conditional probabilities of rockfalls caused by temperature variation (1) with a 1-day aggregation scale during summer between 1000-2000masl and (2) with an aggregation scale of 6 days during spring season below 1000masl are shown. Altitudes between 1000m to 2000m show a probability of 14.3% for rockfalls with temperature variation of -9°C to -6°C. Below 1000m rockfalls are more probable (20%) for temperature range between 8.8°C to 11°C. Temperature variation frequencies do not change significantly over the decades, implying that temperature variation can be considered stable from a climate perspective.

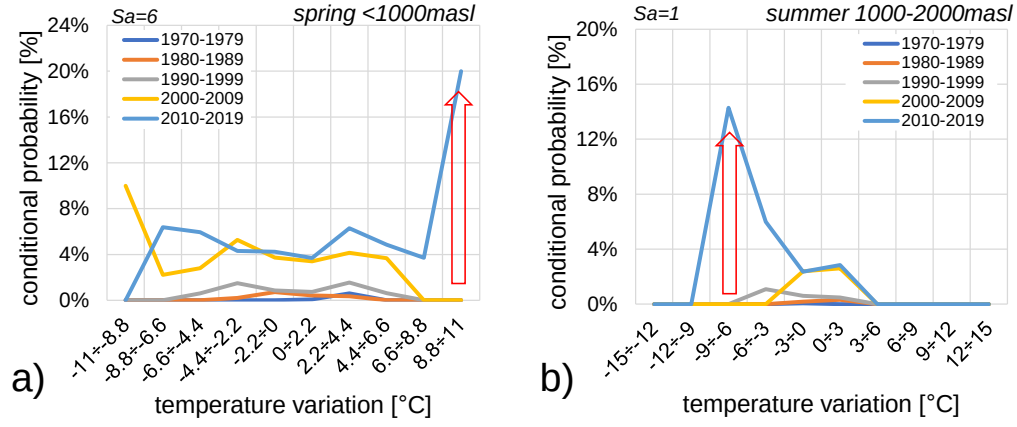

Figure 14: Conditional probabilities from 1970 to 2019 during: (a) summer season between 1000-2000masl and (b) during spring season below 1000m of altitude.

4.3.5 Freeze-Thaw cycle and icing

As the Bayesian analysis for this weather variable relies on three time-series of maximum, mean, and minimum temperatures obtained through regionalization, the results are significantly influenced by this process. To illustrate this, we compare the

https://doi.org/10.5194/egusphere-2024-4122
Preprint. Discussion started: 26 February 2025

results for minimum and mean temperature time-series with a 7-day aggregation scale, focusing on two specific cases: (i) winter at altitudes below 1000 m.a.s.l. (Figure 15) and (ii) spring between 1000 m.a.s.l. and 2000 m.a.s.l. (Figure 16).

Equation (10) shows that the conditional probability of a rockfall event (P(M|R)) depends on the frequency of freeze-thaw cycles (F/T) and icing events. As the conditional probability ranges from 0 to 1, variations in the numerator (i.e., the frequency of F/T and icing events) have a more significant impact on the overall trend of P(M|R) than variations in the denominator. This is particularly evident when F/T and icing events exhibit similar trends over consecutive days.

In Figure 15(a-b), where icing events are more prevalent than F/T cycles, P(M|R) increases with increasing icing events and decreases with increasing F/T cycles. Conversely, in Figure 15(c-d) where F/T cycles are more frequent, the opposite trend is observed.

Similar trends are observed in Figure 16 with the specific behaviour depending on the relative frequency of F/T and icing events. For instance, in Fig. 16(a-b), P(M|R) increases with increasing F/T events and decreases with increasing icing events. The contrasting trends observed in the two examples can be attributed to the varying influence of rockfall probability. Below 1000 m.a.s.l., rockfall probability is relatively stable, while between 1000 m.a.s.l. and 2000 m.a.s.l., it tends to increase over time.

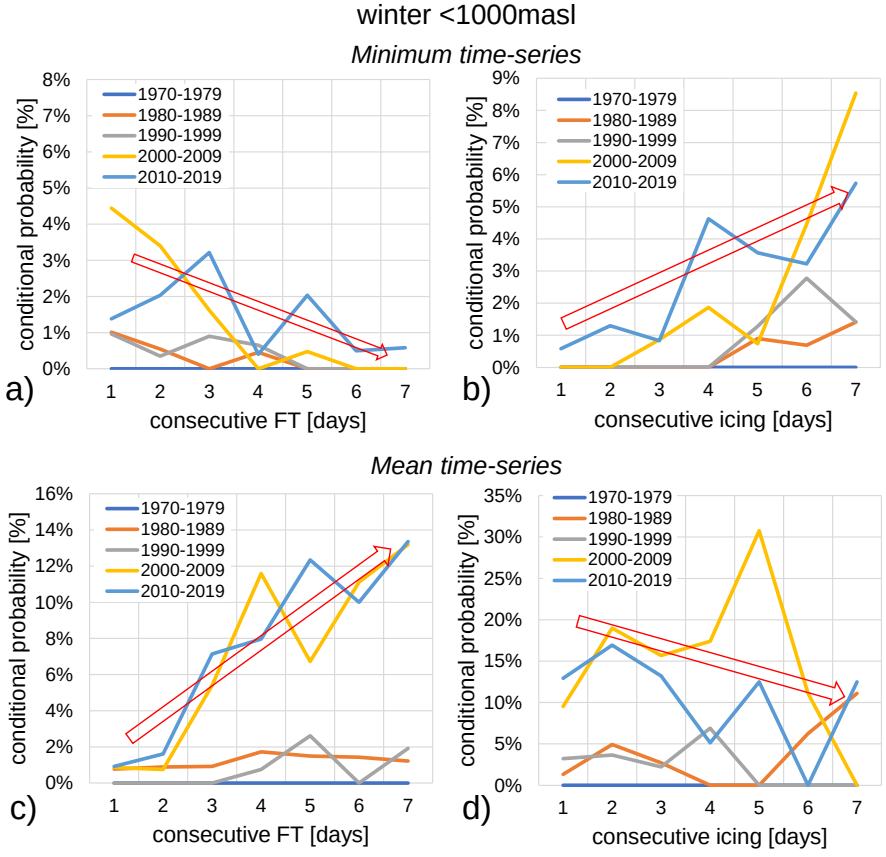

Figure 15: Consecutive probabilities of rockfalls during winter below 1000masl from 1970 to 2019 with an aggregation scale of 7 days. (a and c) trigger by freeze-thaw cycles with minimum and medium times-series. (b and d) trigger by icing with minimum and maximum time-series.

https://doi.org/10.5194/egusphere-2024-4122
Preprint. Discussion started: 26 February 2025

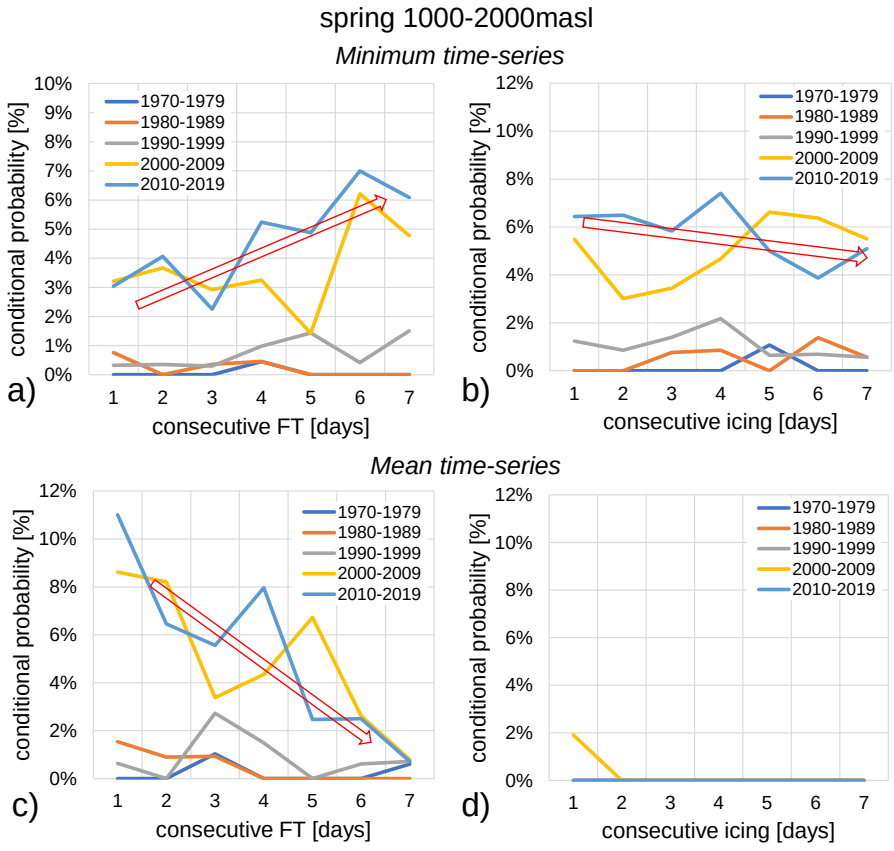

Figure 16: Consecutive probabilities of rockfalls during spring between 1000masl and 2000masl from 1970 to 2019 with an aggregation scale of 7 days. (a and c) trigger by freeze-thaw cycles with minimum and medium times-series. (b and d) trigger by icing with minimum and maximum time-series.

5 Discussion

5.1 Climate

Climate variations have been monitored by many authors in terms of temperature rates over different years. For instance, Gobiet et al. (2014) reported increasing temperature in the alpine region from 1980 onwards, with annual mean warming rates of 0.5°C per decade. They also noted that the 21st-century temperature changes are expected to affect not only rising values but also in seasonal cycles. Similarly, in the Swiss Alps, Allen and Huggel (2013) observed an increase in the values and frequencies of maximum temperature, T_{max}, at a rate of 0.49°C per decade during summer season. Ceppi et al (2012) reported a rate of 0.46 °C/decade, and Beniston (2006) found that winter minimum temperatures, T_{min}, below 1000m elevation increased by about 4°C for the period 1961-1990, while summer temperatures are projected to exceed current values by 5.5–6°C. It is worth noticing that during the Early Twentieth Century Warming (ETCW, 1916-1945) a maximal global warming trend of 0.47°C/30 years was observed (Bengtsson et al., 2004). The climate reports for the study area align with these findings. The ZAMG (2015) show a climate report about a subregion of alpine arch (Tirolo, Altoadige and Belluno). From the results of this report, normal climate fluctuations are presents until 1980, whereas, from 1980 to 2010 is marked a warming trend. Seasonally, the following trends were noted: (i) minimal warming in spring and summer; (ii) less variation in autumn temperatures, (iii) milder winters. Consequently, warm days in summer have increased, while icing or frost days have decreased. Nigrelli and Chiarle (2023) stated that during the most recent normal climatological period (1991-2020), the annual

https://doi.org/10.5194/egusphere-2024-4122
Preprint. Discussion started: 26 February 2025

average minimum temperature was -2.4 °C, with a warming rate of 0.4 °C per decade, and the annual average maximum temperature was 4.4 °C with a warming rate of 0.5 °C per decade. Summer and autumn temperatures showed the highest warming rates, about 0.6 °C per decade. In this study, to calculate temperature annual averages, 12 weather stations with full time-series, were considered in order to observe a trend during time. Since the chosen stations were distributed at different altitudes, two periods were considered to have complete time-series: 1970-2019 for stations below 2000m, and 1985-2019 for stations above 2000m.

Considering all stations and analysing overlapping period from 1985 to 2019, the annual average warming rate for minimum and maximum temperature is 0.28°C per decade and 0.15°C per decade, respectively (Figure 17a). The highest warming rates were found during the spring period with a maximum increase for maximum temperature of about 0.33°C per decade. Analysing stations by altitudes, an annual warming rate of 0.51°C per decade is found above 2000m (Figure 17d); however, for this latter rate, consideration should be given to the shorter period considered. Analysing stations by seasons, maximum temperature warming rate happened, also for this case, during spring season.

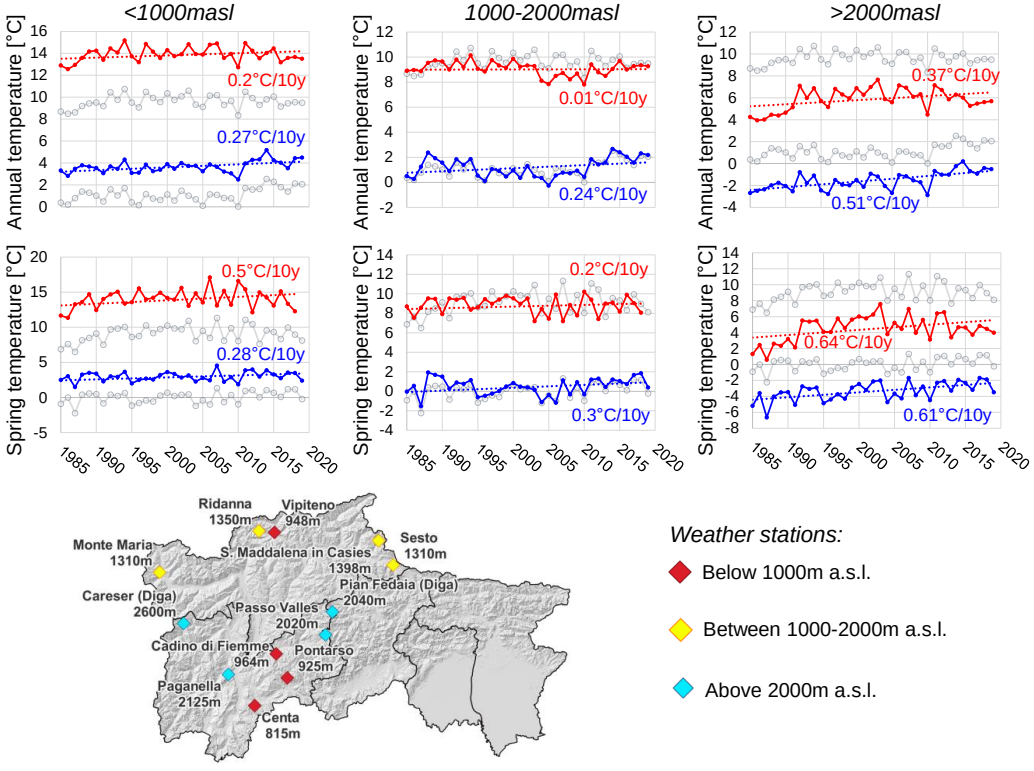

Figure 17: Annual and spring T_{max} and T_{min} trends considering 12 weather stations from 1985 to 2019 for case study; location of weather stations considered are shown below. The maximum and minimum annual and spring values computed by using data of all weather stations are plotted in grey

In this work, an increase in the frequency of high air mean temperatures over the decades is revealed, particularly at altitudes between 1000m and 2000m during the spring season, at all elevation in summer, and below 1000m in autumn, with a 90-day aggregation scale. These results align with the warming trend observed across the entire alpine region by the aforementioned authors.

Water availability in some regions may decline due to reduced precipitation and a decrease in snow-pack and snow season in many mountain regions (Beniston, 2003). In Swiss Alps, at elevations below 1200m, there has been a reduction in the total amount of snow and the duration of the snow season by about 100 days since the mid-1980s. Beniston (2006) noted that for every 1°C increase in temperature, the snowline rises by about 150m. Nigrelli and Chiarle (2023) observed a decrease in the

https://doi.org/10.5194/egusphere-2024-4122
Preprint. Discussion started: 26 February 2025

Alps in the number of icing days (days when the maximum temperature is below 0 °C) by 6 days every decade, and the number of freeze-thaw cycle days (days when the minimum temperature is below 0 °C) by 9 days every decade. Considering the same weather stations used for the calculation of the temperature trends, a decrease of about 7.3 freeze-thaw days and about 2.2 icing days every decade (Figure 18a). From the seasonal analysis, generally the trend is decreasing, however above 2000m FT cycles increase at a rate of 3.3days/10y and 2.7days/10y in winter and spring respectively (Figure 18b-c). In winter above 2000m, a loss of 2.1 ice days per decade is calculated (Figure 18e).

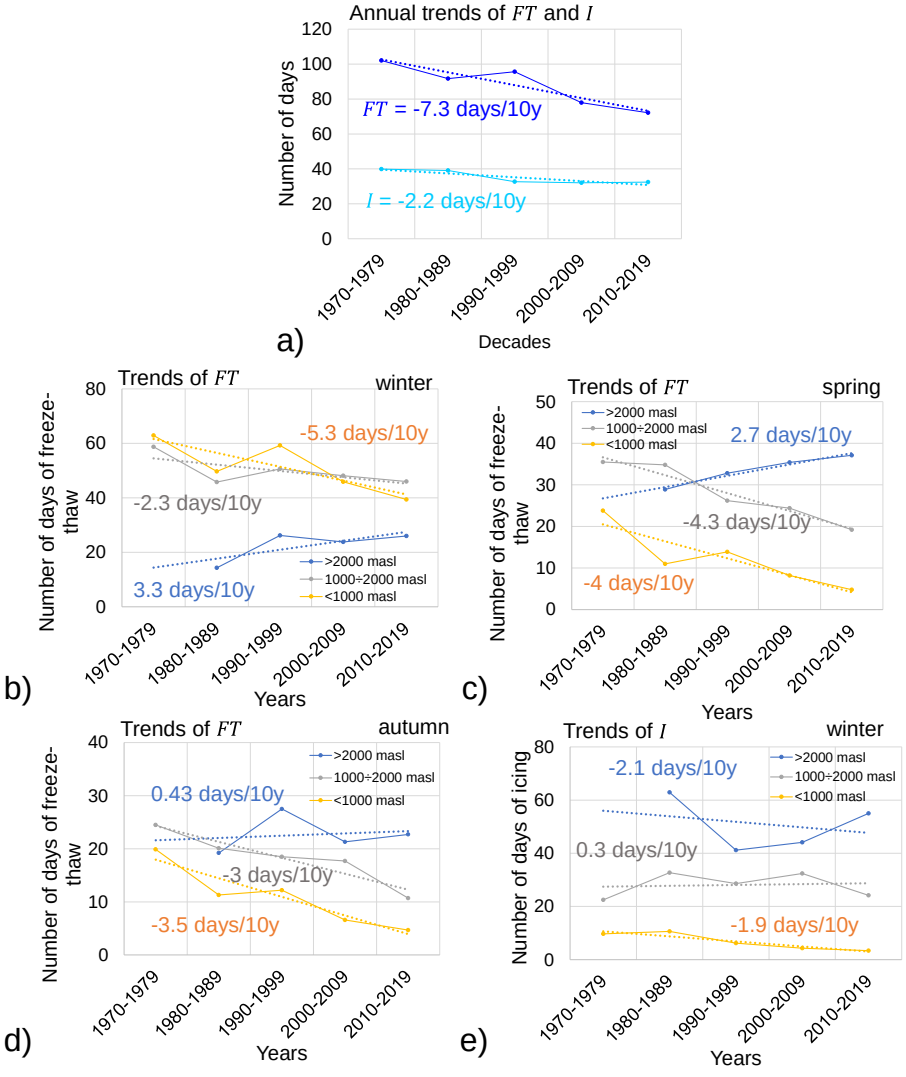

Figure 18: Annual and seasonal freeze-thaw and icing trends regarding to altitudes for this case study during 1970 to 2019. (a) considering 12 weather stations; (b) trends of FT during winter season; (c) trends of FT during spring season; (d) trends of FT during autumn season; (e) trends of I during winter season.

Similar results in terms of reduction in the persistence and frequency of freeze/thaw and icing cycles were also found. Below 2000m, the freeze/thaw cycles persist less and stop earlier in the decades, ceasing in the early spring and reappearing in November. Above 2000m, the frequencies of ice days decrease in May during the last decade, while in October, they appear more frequently but with shorter daily durations, leading to a delay in the onset of the winter season.

https://doi.org/10.5194/egusphere-2024-4122
Preprint. Discussion started: 26 February 2025

Therefore, it can be concluded that springs and autumns are getting warmer, and summers have increasing frequencies of high temperature values, leading to an anticipation of summer and a delayed onset of winter. Indeed, considering the 12 weather stations with full time-series illustrated before, from 1970 to 2019 an increase temperature of about 1.5°C in winter and 3°C in summer is observed (Figure 19a-c). During the spring and autumn seasons, an increase in mean temperature of about 3°C and 2°C respectively, is observed, along with a shift in onset of 30 days for spring and 20 days for autumn, thus causing a change in the length of these two seasons (Figure 19b-d), with a more significant change during spring.

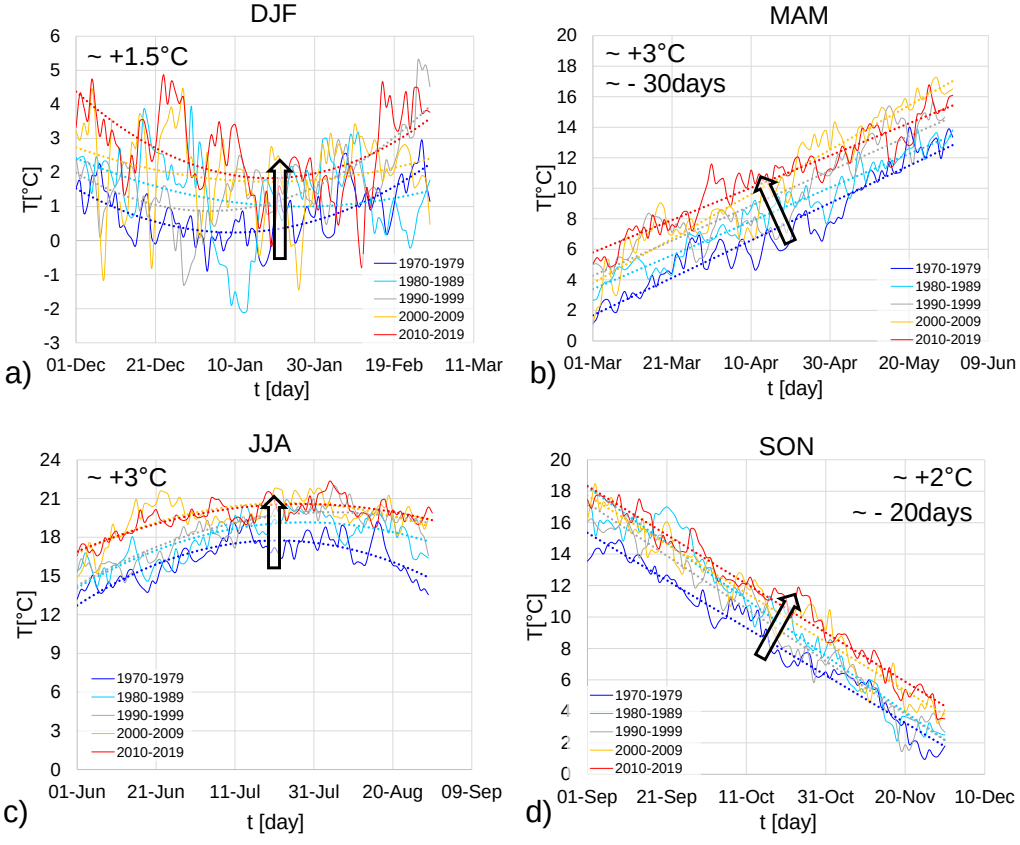

Figure 19: Daily time series of air mean temperature over 1970-2019 during: (a) winter (DJF), (b) spring (MAM), (c) summer (JJA) and (d) autumn seasons (SON).

Wang et al (2021) achieved similar results on a global scale. They observed that between 1952 and 2011, the length of the four seasons changed: spring and summer started earlier by 1.6days/10years and 2.5 days/10years, respectively, while the onset of autumn and winter was delayed by 1.7days/10years and 0.5days/10years, respectively.

Regarding rainfall, the results indicate that high-intensity rainfall events are becoming more frequent, consistent with findings by Schmidli and Frei (2005) and Widmann and Schär (1997), who stated that mean precipitation increased in the 20th century during fall and winter. Beniston (2006) noted that precipitation in the Swiss Alps changed, with winter precipitation decreasing marginally (2–3%) while summer precipitation is projected to decrease by 15–20% in most parts of the alpine chain. According to Christensen and Christensen (2003), reductions in average summer precipitation may be accompanied by a sharp increase in short but heavy precipitation events. Gobiet et al (2014) stated that precipitation decreases in summer and increases in winter. In this work, however, precipitation increases significantly in the winter season, while summer variations are modest over the decades.

https://doi.org/10.5194/egusphere-2024-4122
Preprint. Discussion started: 26 February 2025

To visualize long-term trends changes in climatic records, fluctuations and periodicities in precipitation, Garbrecht and Fernandez (1994) used the Rescaled Adjusted Partial Sums (RAPS).

The Rescaled Adjusted Partial Sums (RAPS) method is a powerful tool for analysing time series data, particularly in hydrology and meteorology. This method supports the detection of irregularities and fluctuations within a time series (e.g., temperature, precipitation) that might not be apparent using traditional analysis techniques. RAPS involves rescaling the partial sums of deviations from the mean of a time series, allowing for the identification of significant changes or trends over time and it helps in visualizing and analysing the cumulative deviations from the mean, rescaled by the standard deviation, to detect underlying patterns and trends in the data. It is particularly effective for identifying breakpoints and subperiods within the data, making it valuable for studying long-term climatic trends and periodicities (Garbrecht and Fernandez, 1994, Durin et al., 2022). Mathematically, the RAPS method can be expressed with the following Eq. (14):

$$RAPS_k \sum_{t=1}^{k} \frac{Y_t - \bar{Y}}{S_y} \quad (14)$$

Where $RAPS_k$ is the rescaled adjusted partial sum at time $(t = 1,2,..,k)$ represents the individual data points in the time series, $\bar{Y}$ is the mean of the time series, and S_y is the standard deviation of the time series.

Garbrecht and Fernandez (1994) studied 90-year annual rainfall (1902-1991) in Bryan County, Oklahoma and found two major trends: a general decrease from 1902 to 1966, followed by an increase from 1967 to 1991. This application shows occurrences of floods and droughts events defined by fluctuations in the RAPS.

In this work, RAPS analysis by altitude, was performed considering the 12 meteorological stations (Figure 20). Below 1000m a general decrease from 1985 to 2008 was observed, followed by an increasing trend. During autumn, many fluctuations were observed. In 2002, a sharp increase is noted, likely corresponding to high rainfall events in May and November (Bollettino meteorologico e valanghe, Ufficio idrografico di Bolzano; Protezione Civile Provincia Autonoma di Trento). Between 1000m and 2000m, the trend is decreasing because time-series remains below the mean value until 2005. After this date, an increment is observed in RAPS. Above 2000m, a general decrease until 2006 was recorded, followed by an increasing trend. During spring, many fluctuations were observed.

https://doi.org/10.5194/egusphere-2024-4122
Preprint. Discussion started: 26 February 2025

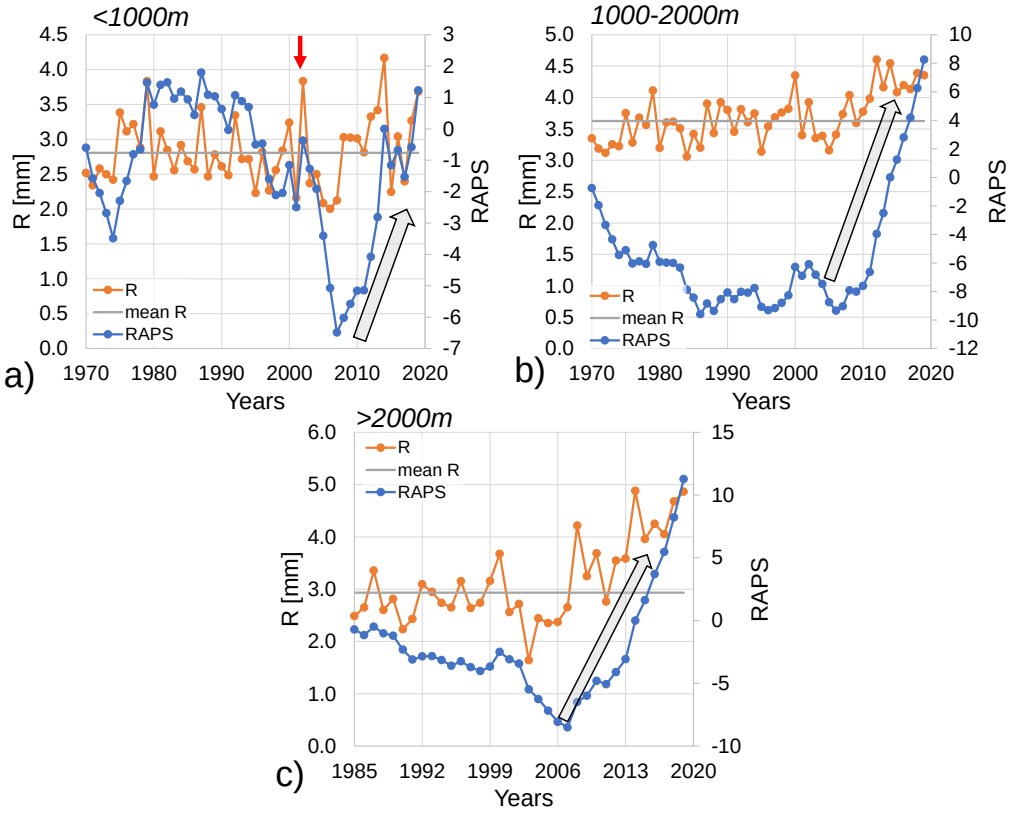

Figure 20: Annual mean rainfall values and Rescaled Adjusted Partial Sums: (a) below 1000m from 1970 to 2019; (b) between 1000-2000m from 1970 to 2019; (c) above 2000m from 1985 to 2019. The red arrow shows extraordinary events of 2002.

5.2 Rockfall

Rockfall frequency exhibits seasonal variability. Previous studies in the Alps have reported diverse seasonal patterns: Coro et al. (2015) identified peaks in October-November, June-July, and March; Bajni et al. (2021) observed peaks in spring and minor peaks in January in the Aosta Valley; Frayssines and Hantz (2006) found a primary peak in winter and a secondary peak in April in the French Alps; and Perret et al. (2006) noted seasonality in early spring in the Swiss Alps. This study similarly reveals peaks in November, February, April, and August.

Climate variables significantly influence rockfall occurrence. A strong correlation exists between winter rockfalls and precipitation, particularly daily rainfall events exceeding 31.5 mm. Summer rockfalls above 2000 m are potentially linked to mean air temperatures exceeding 9°C, while spring rockfalls between 1000 m and 2000 m correlate with mean air temperatures ranging from 5.8°C to 15.4°C. Additionally, rockfalls exhibit a correlation with winter temperature amplitudes between 1°C and 7°C at elevations between 1000 m and 2000 m and summer temperature amplitudes between 10.8°C and 12°C above 2000 m.

Air temperature plays a crucial role in rockfall initiation, particularly during warmer months. Elevated temperatures can accelerate snowmelt, infiltrating rockwall discontinuities and triggering rockfall, especially at the onset of summer and autumn (Allen and Huggel, 2013). Furthermore, air temperature influences other critical mechanisms such as icing and freeze-thaw cycles (Noetzli et al., 2003; Salzmann et al., 2007; Manent et al., 2024).

The impact of freeze-thaw (FT) cycles on rockfall occurrence has been previously investigated. Frayssines-Hantz (2006) observed a correlation between rockfalls and frequent temperature fluctuations around the freezing point in early spring and

https://doi.org/10.5194/egusphere-2024-4122
Preprint. Discussion started: 26 February 2025

late autumn at elevations between 1000 m and 2000 m. D'Amato et al. (2016) reported an increase in rockfall frequency during freeze-thaw episodes, particularly during thawing periods. This study confirms these findings, with increased rockfall frequency observed in winter below 1000 m during FT cycles lasting 1 to 3 days and in spring between 1000 m and 2000 m. A slight increase in rockfall frequency was also observed during icing periods lasting 1 to 5 days.

The methodology employed in this study for obtaining the sampled time-series was inspired by Paranunzio et al. (2015). Consequently, a comparison of frequency and anomaly results with those reported by Paranunzio et al. (2015) is essential. Paranunzio et al. (2015) concluded that four out of five case studies in Piedmont could be attributed to meteorological anomalies, such as temperature rise or heavy precipitation. In a subsequent study, Paranunzio et al. (2016) found that in 85% of cases across the Western and Eastern Alps, at least one climate anomaly was associated with rockfall occurrence, with most events linked to short-term temperature anomalies. Precipitation was identified as a contributing factor in only 15% of rockfall events at weekly, monthly, and quarterly aggregation scales.

The method of Paranunzio et al. (2016) was adapted and tested in this study, and the results were compared with those obtained using the proposed method. The same climate variables (mean air temperature, temperature variations over different days, and precipitation) were analyzed at identical aggregation scales (daily, weekly, monthly, and quarterly) for ΔT 1, 3, and 6 days prior to the event. The non-exceedance probability P(V) was calculated with a significance level (α=0.2).

The results indicate that 50% of rockfalls were associated with at least one anomaly. Positive temperature anomalies were more frequent than precipitation anomalies (Fig. 21). Daily and weekly temperature anomalies were more frequently cold (negative) than hot (positive), while monthly and quarterly anomalies were more frequently hot than cold. Regarding the season of occurrence, rockfalls were slightly more frequent in autumn (for positive anomalies) and spring (for negative anomalies). All anomalies were more frequent below 1000 m asl, and small events (<100m3) predominated. Conversely, large-magnitude events were more frequent with positive anomalies. Finally, numerous events occurred in non-permafrost areas, while in permafrost areas, rockfalls were more strongly controlled by permafrost-favorable conditions than other factors.

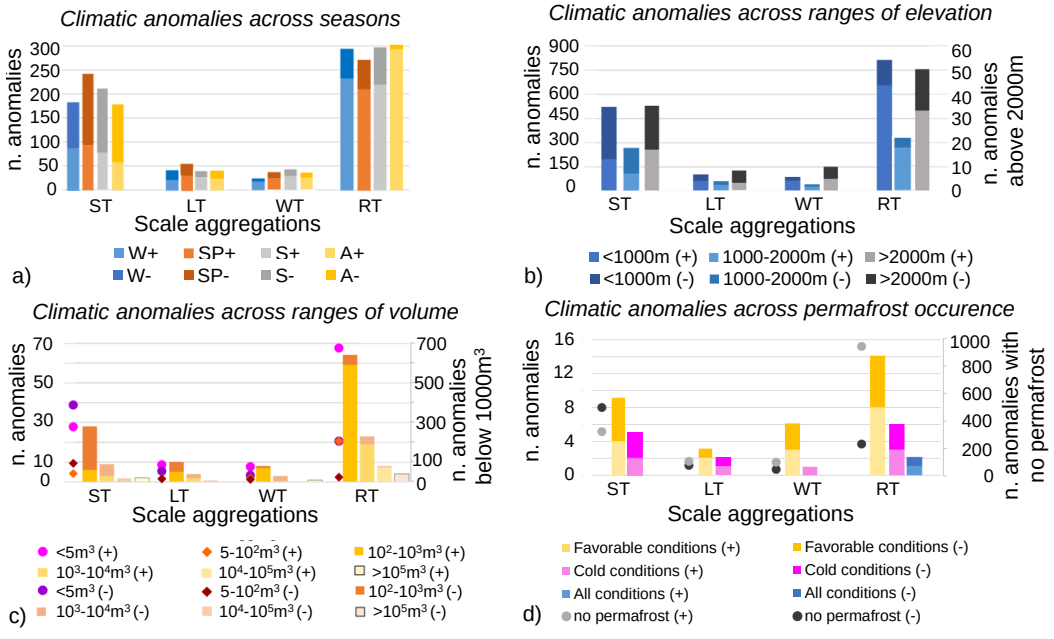

Figure 21: Distribution of rockfalls according to controlling factors and aggregation scales: (a) season of occurrence (W=winter; SP=spring; S=summer; A=autumn); (b) range of elevation; (c) range of volume; (d) expected permafrost occurrence in detachment zone. The aggregation scales are: ST= short-term temperature; LT= long-term temperature; WT= widespread temperature; R= precipitations. Positive anomalies are assigned with (+) and negative with (-).

https://doi.org/10.5194/egusphere-2024-4122
Preprint. Discussion started: 26 February 2025

6 Conclusion

This study confirms a significant warming trend in the alpine region, consistent with previous research by analysing data from 1970 to 2019. The annual mean warming rate from 1985-2019 for the study area is recorded for minimum temperature at 0.28°C per decade and for maximum temperature at 0.15°C per decade. Notably, the highest warming rates were observed during the spring period, with a maximum increase of about 0.33°C per decade. Springs and autumns are getting warmer, summers are experiencing increasing frequencies of high temperature values, and winters are becoming milder. This leads to an earlier onset of summer and a delayed onset of winter, altering the length of these seasons.

Significant changes in precipitation patterns were observed, with an increase in high-intensity rainfall events, particularly in winter, while a reduction in low-intensity rainfall was recorded across all seasons. This finding aligns with observations in the literature for the Alpine region. Conversely, summer precipitation variations were modest, contrasting with some previous projections.

A notable decline in icing and freeze-thaw cycles days are observed, specifically is estimated a decrease of 7.3 days of freeze-thaw cycles and 2.2 days of icing every decade.

The Rescaled Adjusted Partial Sums (RAPS) method provided valuable insights into long-term trends and fluctuations in precipitation highlighting that climate evolution is not due to the variation of the maximum values of the climate variables but rather a variation in their frequencies over the years.

Rockfall analysis showed that rockfall frequencies have three main peaks in November, February-April, and August. In terms of the aspect of the source area, below 1000m.a.s.l., 70% of rockfalls have south-facing slopes; between 1000-2000m.a.s.l., 35% have south-east facing slopes; and above 2000m, 50% of events have north-northwest facing slopes, possibly due to permafrost thawing.

Rockfalls and high intensity rainfall are correlated in autumn with monthly and quarterly rainfalls with 12.4% below1000m and 22.2% at altitude between 1000m and 2000m; a correlation with air mean temperatures of 12.7% within range from 21°C to 24°C during summer season between 1000m and 2000m at weekly scale is observed and increment conditional probability reaches 2.2% above 2000m with a range of temperature from 17.6°C to 20.8°C during autumn season with Sa=30.

Rockfalls are correlated with temperature amplitude in spring below 1000m.a.s.l. from 8.8°C to 9.9°C with 28.6% of probability and in winter between 1000masl and 2000m.a.s.l. in the range of 9°C to 10°C with 5.8% of probability. According to temperature variation, rockfalls happen in summer between 1000m and 2000m are correlated with 14.3% with a temperature variation of -9°C to -6°C and during spring season below 1000masl with a conditional probability of 20% with maximum range of variation (8.8°C÷11°C).

From the analysis of correlation between rockfall events with freeze-thaw cycles and icing periods, it is observed how the probability results change depending on the calculated timeseries (maximum, average, minimum).

Author contributions

FB: meteorological and rockfall data collection and analysis; FB and GD performed the statistical analyses; FB, GD and GC prepared the draft manuscript. PF and GC provided funding, supervised the project and the analyses.

Competing interests

The authors declare that they have no conflict of interest.

https://doi.org/10.5194/egusphere-2024-4122
Preprint. Discussion started: 26 February 2025

References

Allen, S., and Huggel, C.: Extremely warm temperatures as a potential cause of recent high mountain rockfall. Global and Planetary Change, 107, 59-69, 2013.

Bajni, G., Camera, C. A., and Apuani, T.: Deciphering meteorological influencing factors for Alpine rockfalls: a case study in Aosta Valley. Landslides, 18(10), 3279-3298, 2021.

Bassetti, M., and Borsato, A.: Evoluzione geomorfologica della Bassa Valle dell'Adige dall'Ultimo Massimo Glaciale: sintesi delle conoscenze e riferimenti ad aree limitrofe. Acta Geologica, 82(31), e42, 2005.

Bayes, R. T.: Bayes' Theorem. An essay towards solving a problem in the doctrine of chances, Philosophical, 370-418, 1763.

Bengtsson, L., Semenov, V. A., and Johannessen, O. M.: The early twentieth-century warming in the Arctic—A possible mechanism. Journal of Climate, 17(20), 4045-4057, 2004.

Beniston, M.: Climatic change in mountain regions: a review of possible impacts. Climatic change, 59(1), 5-31, 2003.

Beniston, M.: Mountain weather and climate: a general overview and a focus on climatic change in the Alps. Hydrobiologia, 562, 3-16, 2006.

Berti, M., Martina, M. L. V., Franceschini, S., Pignone, S., Simoni, A., and Pizziolo, M.: Probabilistic rainfall thresholds for landslide occurrence using a Bayesian approach. Journal of Geophysical Research: Earth Surface, 117(F4), 2012.

Böhm, R., Auer, I., Brunetti, M., Maugeri, M., Nanni, T., and Schöner, W.: Regional temperature variability in the European Alps: 1760–1998 from homogenized instrumental time series. International Journal of Climatology: A Journal of the Royal Meteorological Society, 21(14), 1779-1801, 2001.

Bosellini, A., Gianolla, P., and Stefani, M.: Geology of the Dolomites. Episodes Journal of International Geoscience, 26(3), 181-185, 2003.

Brunetti, M., Lentini, G., Maugeri, M., Nanni, T., Auer, I., Bohm, R., and Schoner, W.: Climate variability and change in the Greater Alpine Region over the last two centuries based on multi-variable analysis. International Journal of Climatology, 29(15), 2197-2225, 2009.

Bunce, C. M., Cruden, D. M., and Morgenstern, N. R.: Assessment of the hazard from rock fall on a highway. Canadian Geotechnical Journal, 34(3), 344-356, 1997.

Ceppi, P., Scherrer, S. C., Fischer, A. M., and Appenzeller, C.: Revisiting Swiss temperature trends 1959–2008. International Journal of Climatology, 32(2), 203-213, 2012.

Christensen, J. H., and Christensen, O. B., Severe summertime flooding in Europe. Nature, 421(6925), 805-806, 2003.

Corò, D., Galgaro, A., Fontana, A., and Carton, A.: A regional rockfall database: the Eastern Alps test site. Environmental Earth Sciences, 74, 1731-1742, 2015.

Courtial-Manent, L., Ravanel, L., Mugnier, J. L., Deline, P., Lhosmot, A., Rabatel, A., ... and Batoux, P.: 18-years of high-Alpine rock wall monitoring using terrestrial laser scanning at the Tour Ronde east face, Mont-Blanc massif. Environmental Research Letters, 19(3), 034037, 2024.

Crosta, G. B., and Agliardi, F.: Parametric evaluation of 3D dispersion of rockfall trajectories. Natural Hazards and Earth System Sciences, 4(4), 583-598, 2004.

Dal Piaz, G. V., Bistacchi, A., and Massironi, M.: Geological outline of the Alps. Episodes Journal of International Geoscience, 26(3), 175-180, 2003.

Davies, M. C., Hamza, O., and Harris, C.: The effect of rise in mean annual temperature on the stability of rock slopes containing ice-filled discontinuities. Permafrost and periglacial processes, 12(1), 137-144, 2001.

Delonca, A., Gunzburger, Y., and Verdel, T.: Statistical correlation between meteorological and rockfall databases. Natural Hazards and Earth System Sciences, 14(8), 1953-1964, 2014.

Doglioni, C.: Tectonics of the Dolomites (southern Alps, northern Italy). Journal of structural geology, 9(2), 181-193, 1987.

https://doi.org/10.5194/egusphere-2024-4122
Preprint. Discussion started: 26 February 2025

Douglas, G. R.: Magnitude frequency study of rockfall in Co. Antrim, N. Ireland. Earth Surface Processes, 5(2), 123-129, 1980.

Draebing, D., and Krautblatter, M.: The efficacy of frost weather processes in alpine rockwalls. Geophysical Research Letters, 46(12), 6516-6524, 2019.

Đurin, B., Kranjčić, N., Kanga, S., Singh, S. K., Sakač, N., Pham, Q. B., ... and Di Nunno, F.: Application of Rescaled Adjusted Partial Sums (RAPS) method in hydrology–an overview. Advances in civil and architectural engineering, 13(25), 58-72, 2022.

Fischer, L., Kääb, A., Huggel, C., and Noetzli, J.: Geology, glacier retreat and permafrost degradation as controlling factors of slope instabilities in a high-mountain rock wall: the Monte Rosa east face. Natural Hazards and Earth System Sciences, 6(5), 761-772, 2006.

Frattini, P., Crosta, G., Carrara, A., and Agliardi, F.: Assessment of rockfall susceptibility by integrating statistical and physically-based approaches. Geomorphology, 94(3-4), 419-437, 2008.

Frayssines, M., and Hantz, D.: Failure mechanisms and triggering factors in calcareous cliffs of the Subalpine Ranges (French Alps). Engineering Geology, 86(4), 256-270, 2006.

Garbrecht, J., and Fernandez, G. P.: Visualization of trends and fluctuations in climatic records 1. JAWRA Journal of the American Water Resources Association, 30(2), 297-306, 1994.

Gariano, S. L., and Guzzetti, F.: Landslides in a changing climate. Earth-science reviews, 162, 227-252, 2016.

Gobiet, A., Kotlarski, S., Beniston, M., Heinrich, G., Rajczak, J., and Stoffel, M.: 21st century climate change in the European Alps—A review. Science of the total environment, 493, 1138-1151, 2014.

Gruber, S., and Haeberli, W.: Permafrost in steep bedrock slopes and its temperature-related destabilization following climate change. Journal of Geophysical Research: Earth Surface, 112(F2), 2007.

Hilker, N., Badoux, A., and Hegg, C.: The Swiss flood and landslide damage database 1972–2007. Natural Hazards and Earth System Sciences, 9(3), 913-925, 2009.

Huggel, C., Allen, S., Deline, P., Fischer, L., Noetzli, J., and Ravanel, L.: Ice thawing, mountains falling—are alpine rock slope failures increasing?. Geology Today, 28(3), 98-104, 2012.

Krautblatter, M., and Moser, M.: A nonlinear model coupling rockfall and rainfall intensity based\newline on a four year measurement in a high Alpine rock wall (Reintal, German Alps). Natural Hazards and Earth System Sciences, 9(4), 1425-1432, 2009.

Krautblatter, M., Funk, D. and Günzel, F. K.: Why permafrost rocks become unstable: a rock–ice-mechanical model in time and space. Earth Surf. Process. Landf. 38, 876–887, 2013.

Letortu, P.: Le recul des falaises crayeuses haut-normandes et les inondations par la mer en Manche centrale et orientale: de la quantification de l'aléa à la caractérisation des risques induits (Doctoral dissertation, Université de Caen), 2013.

Luethi, R., Gruber, S. and Ravanel, L.: Modelling transient ground surface temperatures of past rockfall events: towards a better understanding of failure mechanisms in changing periglacial environments. Geogr. Ann. Ser. A Phys. Geogr. 97, 753–767, 2015.

Macciotta, R., Hendry, M., Cruden, D. M., Blais-Stevens, A., and Edwards, T.: Quantifying rock fall probabilities and their temporal distribution associated with weather seasonality. Landslides, 14(6), 2025-2039, 2017.

Macciotta, R., Martin, C. D., Edwards, T., Cruden, D. M., and Keegan, T.: Quantifying weather conditions for rock fall hazard management. Georisk: assessment and management of risk for engineered systems and geohazards, 9(3), 171-186, 2015.

Matsuoka, N., and Sakai, H.: Rockfall activity from an alpine cliff during thawing periods. Geomorphology, 28(3-4), 309-328, 1999.

Noetzli, J., Hoelzle, M., and Haeberli, W.: Mountain permafrost and recent Alpine rock-fall events: a GIS-based approach to determine critical factors. In Proceedings of the 8th International Conference on Permafrost (Vol. 2, pp. 827-832). Zürich: Swets & Zeitlinger Lisse, 2003.

https://doi.org/10.5194/egusphere-2024-4122
Preprint. Discussion started: 26 February 2025

Noetzli, J., and Gruber, S.: Transient thermal effects in Alpine permafrost. The Cryosphere, 3(1), 85-99, 2009.

Palau, R. M., Gisnås, K. G., Solheim, A., and Gilbert, G. L.: Regional-scale analysis of weather-related rockfall triggering mechanisms in Norway, and its sensitivity to climate change. *Natural Hazards and Earth System Sciences Discussions*, *2024*, 1-27, 2024.

Palladino, M. R., Viero, A., Turconi, L., Brunetti, M. T., Peruccacci, S., Melillo, M., ... and Guzzetti, F.: Rainfall thresholds for the activation of shallow landslides in the Italian Alps: the role of environmental conditioning factors. Geomorphology, 303, 53-67, 2018.

Paranunzio, R., and Marra, F.: Open gridded climate datasets can help investigating the relation between meteorological anomalies and geomorphic hazards in mountainous areas. Global and Planetary Change, 232, 104328, 2024.

Paranunzio, R., Chiarle, M., Laio, F., Nigrelli, G., Turconi, L. and Luino, F.: New insights in the relation between climate and slope failures at high-elevation sites. Theoretical and Applied Climatology, 137:1765-1784, 2019.

Paranunzio, R., Laio, F., Chiarle, M., Nigrelli, G. and Guzzetti, F.: Climate anomalies associated with the occurence of rockfalls at high-elevation in the Italian Alps, 2016.

Paranunzio, R., Laio, F., Nigrelli, G., and Chiarle, M.: A method to reveal climatic variables triggering slope failures at high elevation. Natural Hazards, 76, 1039-1061, 2015.

Pepin, N. C., Arnone, E., Gobiet, A., Haslinger, K., Kotlarski, S., Notarnicola, C., ... and Adler, C.: Climate changes and their elevational patterns in the mountains of the world. Reviews of Geophysics, 60(1), e2020RG000730, 2022.

Perret, S., Stoffel, M., and Kienholz, H.: Spatial and temporal rockfall activity in a forest stand in the Swiss Prealps—a dendrogeomorphological case study. Geomorphology, 74(1-4), 219-231, 2006.

Ravanel, L., Magnin, F. and Deline, P. Impacts of the 2003 and 2015 summer heatwaves on permafrost-affected rock-walls in the Mont Blanc massif. Sci. Total Environ. 609, 132–143, 2017.

Rupp, S., and Damm, B.: A national rockfall dataset as a tool for analysing the spatial and temporal rockfall occurrence in Germany. Earth Surface Processes and Landforms, 45(7), 1528-1538, 2020.

Salzmann, N., Nötzli, J., Hauck, C., Gruber, S., Hoelzle, M., and Haeberli, W.: Ground surface temperature scenarios in complex high-mountain topography based on regional climate model results. Journal of Geophysical Research: Earth Surface, 112(F2), 2007.

Sandersen, F., Bakkehøi, S., Hestnes, E., and Lied, K.: The influence of meteorological factors on the initiation of debris flows, rockfalls, rockslides and rockmass stability. Publikasjon-Norges Geotekniske Institutt, 201, 97-114, 1997.

Sass, O., and Oberlechner, M.: Is climate change causing increased rockfall frequency in Austria?. Natural Hazards and Earth System Sciences, 12(11), 3209-3216, 2012.

Scavia, C., Barbero, M., Castelli, M., Marchelli, M., Peila, D., Torsello, G., and Vallero, G.: Evaluating rockfall risk: Some critical aspects. Geosciences, 10(3), 98, 2020.

Schär, C., Vidale, P. L., Lüthi, D., Frei, C., Häberli, C., Liniger, M. A., and Appenzeller, C.: The role of increasing temperature variability in European summer heatwaves. Nature, 427(6972), 332-336, 2004.

Schmidli, J., and Frei, C.: Trends of heavy precipitation and wet and dry spells in Switzerland during the 20th century. International Journal of Climatology: A Journal of the Royal Meteorological Society, 25(6), 753-771, 2005.

Stoffel, M., and Huggel, C.: Effects of climate change on mass movements in mountain environments. Progress in physical geography, 36(3), 421-439, 2012.

Stoffel, M., Trappmann, D. G., Coullie, M. I., Ballesteros Cánovas, J. A., and Corona, C.: Rockfall from an increasingly unstable mountain slope driven by climate warming. Nature Geoscience, 17(3), 249-254, 2024.

Stull, R. B.: Meteorology for scientists and engineers: a technical companion book with Ahrens' Meteorology Today, 2000.

Valagussa, A., Frattini, P., and Crosta, G. B.: Earthquake-induced rockfall hazard zoning. Engineering Geology, 182, 213-225, 2014.

https://doi.org/10.5194/egusphere-2024-4122
Preprint. Discussion started: 26 February 2025

Varnes, D. J.: Slope movement types and processes. Special report, 176, 11-33, 1978.

Viani, C., Chiarle, M., Paranunzio, R., Merlone, A., Musacchio, C., Coppa, G. and Nigrelli, G.: An integrated approach to investigate climate-driven rockfall occurence in high alpine slope: the Bessanese glacial basin, Western Italian Alps. Journal of Mountain Sience 17(11), 2020.

Volkwein, A., Schellenberg, K., Labiouse, V., Agliardi, F., Berger, F., Bourrier, F., ... and Jaboyedoff, M.: Rockfall characterisation and structural protection–a review. Natural Hazards and Earth System Sciences, 11(9), 261, 2011.

Wang, J., Guan, Y., Wu, L., Guan, X., Cai, W., Huang, J., ... and Zhang, B.: Changing lengths of the four seasons by global warming. Geophysical Research Letters, 48(6), e2020GL091753.7-2651, 2021.

Widmann, M., and Schär, C.: A principal component and long-term trend analysis of daily precipitation in Switzerland. International Journal of Climatology: A Journal of the Royal Meteorological Society, 17(12), 1333-1356, 1997.

World Meteorological Organization.: Calculation of monthly and annual 30-year standard normals. WCDP 10, WMO-TD 341, 1989.

Zhao, T., Crosta, G.B., Utili, S., and De Blasio F.V.: Investigation of rock fragmentation during rockfalls and rock avalanches via 3-D discrete element analyses. J. Geophys. Res. Earth Surf., 122, 678-695, 2017.